Lisa Bindhofer, BSc

Microalgal microbiome and optimization of heterotrophic cultivation

MASTER'S THESIS

to achieve the university degree of

Diplom-Ingenieurin

Master's degree programme: Biotechnology

submitted to

Graz University of Technology

Supervisor

Univ.-Prof. Dipl.-Biol. Dr.rer.nat. Gabriele Berg

Institute of Environmental Biotechnology

Graz University of Technology

Graz, Juni 2018

AFFIDAVIT

I declare that I have authored this thesis independently, that I have not used other than the declared sources/resources, and that I have explicitly indicated all material which has been quoted either literally or by content from the sources used. The text document uploaded to TUGRAZonline is identical to the present master‘s thesis.

Date

Signature

ACKNOWLEDGEMENT

First and foremost, I would like to thank Univ.-Prof. Dr.rer.nat. Gabriele Berg, my supervisor at the Institute of Environmental Biotechnology, for her professional support throughout the work on my master thesis. She allowed me to get an insight into and understanding of the field of microbiome research. I also want to thank Dr.techn. Tomislav Cernava and Dipl.-Ing. Lisa Krug for their patience and guidance during my work and writing of this thesis. Without their ideas and suggestions, this work would have not been possible.

A special thanks to BDI – BioEnergy International GmbH for enabling me to do parts of my master thesis at the company under the guidance of Dr. Peter Pucher and Dipl.-Ing. Corinna Jäger. They supported me in answering scientific questions and encouraged me continuously during the work of my master thesis.

Thank you to everybody who helped and supported me doing this work. I want to thank colleagues of the Institute of Environmental Biotechnology as well as the company BDI – BioEnergy International GmbH.

Finally yet importantly, I would like to thank my family, especially my parents, for their unconditional encouragement throughout all the years of my education. I am deeply grateful for their continuous support.

Thank you.

Dankeschön.

ABSTRACT

Microalgae are photosynthetically active eukaryotic microorganisms with industrial relevance. Their biotechnological potential has been proven in various publications and studies. The focus of this thesis was centered on the characterization of the eukaryotic microbiome of microalgae in natural habitats and the cultivation optimization of *Chlorella vulgaris* and *Schizochytrium mangrovei.*

It is well known that certain microorganisms can promote the growth of plants. To test if this concept is also applicable to microalgae, information about their natural microbiome is required. In this thesis the microbiomes of different microalgal habitat samples were analyzed with an amplicon study and specific marker genes. Here, the 18S rRNA gene fragment was specifically targeted and sequenced (Illumina MiSeq/HiSeq). A QIIME-based pipeline was used for the analysis of the sequencing results. The bioinformatic evaluation showed similarities in the microbial composition of water samples, independent of the sampling location. The microbiome of the snowfield samples varied with sampling location and the color of the sampling spot, with fungi and *Chlorophyta* as most present on order level. Urban habitats revealed high similarities between each other with the most abundant order *Chlorophyta*. The results can be used for further microbiome comparisons and as a basis for the identification of growth promoting microorganisms.

The nutrient rich biomass of *Chlorella vulgaris* and the omega-3-fatty acid rich lipid of *Schizochytrium mangrovei* can be financially valuable, which makes them relevant for potential industrial applications. Literature shows that very high biomass concentrations are obtainable with heterotrophic cultivation. Therefore, the heterotrophic cultivation of two algae strains was analyzed first with flask experiments and then with lab-scale fermentation experiments. The cultivation conditions were optimized to maximize the biomass concentration, biomass productivity, growth rate and yield. With the optimization of glucose inputs in the cultivation of *Chlorella vulgaris*, a 6 % increase in biomass concentration and a 60 % increased growth rate were observed. Additionally, the yield and biomass productivity were nearly tripled. For *Schizochytrium mangrovei* the biomass concentration was increased by 12 % and a 10 times higher growth rate was achieved, after optimizing the nutrient concentrations. The biomass productivity increased tenfold whereas the yield almost quadrupled. The batch fermentations of *Chlorella vulgaris* revealed a high sensitivity of the cells to stirrer induced shear forces. Lower key indicators than observed in the flask experiments were obtained as a result of unideal

regulation of the oxygen saturation. In contrast, the batch fermentations of *Schizochytrium mangrovei* resulted in a nutrient limitation due to the heat sterilization of the medium, which was confirmed by airlift bioreactor experiments. Analysis of the *Schizochytrium mangrovei* lipid revealed an average lipid content of 45 % with high content of Docosahexaenoic acid (DHA). Overall, the results gained from the conducted experiments showed that heterotrophic cultivation of those two microalgae is a promising approach for industrial use. By further optimization the key indicators can be increased more.

ZUSAMMENFASSUNG

Mikroalgen sind fotosynthetisch aktive eukaryotische Mikroorganismen mit hoher Relevanz für industrielle Anwendungen. Ihr biotechnologisches Potenzial wurde in vielzähligen Publikationen und Studien nachgewiesen. Der Fokus dieser Arbeit lag auf der Charakterisierung des eukaryotischen Mikrobioms von Mikroalgen in natürlichen Lebensräumen und der Kultivierungsoptimierung von *Chlorella vulgaris* und *Schizochytrium mangrovei*.

Wie aus der Fachliteratur ersichtlich ist, können manche Mikroorganismen das Pflanzenwachstum fördern. Um zu überprüfen, ob dieses Konzept auch auf Mikroalgen anwendbar ist, sind Informationen zum natürlichen Mikrobiom dieser Organismen notwendig. In dieser Arbeit wurden verschiedene Lebensraumproben von Mikroalgen mittels einer Amplikon-Studie und spezifischen Markergenen analysiert. Das 18S rRNA Genfragment wurde amplifiziert und sequenziert (Illumina MiSeq/HiSeq). Die gängige Analyseplattform QIIME wurde für die Analyse der Sequenzen benutzt. Bioinformatische Auswertungen zeigten Ähnlichkeiten in der Mikrobiomzusammensetzung von Wasserproben, unabhängig vom Ort der Probenahme. Das Mikrobiom der Schneefeldproben zeigte hohe Variationen, die mit dem Ort der Probenahme und der Färbung des Schneefelds korrelierten. Unterschiedliche Taxa die Pilzen zugeordnet wurden und *Chlorophyta* auf der taxonomischen Rangstufe Ordnung wurden am häufigsten identifiziert. Urbane Lebensräume zeigten eine hohe Ähnlichkeit untereinander, mit hoher Präsenz von *Chlorophyta*. Diese Resultate können für vertiefende Mikrobiomanalysen und als Grundlage für die Identifizierung wachstumsfördernder Mikroorganismen genutzt werden.

Die nährstoffreiche Biomasse von *Chlorella vulgaris* und die Omega-3-Fettsäure reiche Lipidfraktion von *Schizochytrium mangrovei* sind ökonomisch wertvoll, was sie für potenzielle industrielle Anwendungen sehr interessant macht. Es wird in mehreren Literaturstellen berichtet, dass mit heterotropher Kultivierung sehr hohe Biomassekonzentrationen erreicht werden können. Deshalb wurde die heterotrophe Kultivierung von zwei Algenstämmen zuerst mit Kolbenversuchen und dann mit Fermentationsversuchen im Labormaßstab untersucht. Die Kultivierungsbedingungen wurden optimiert, um die Biomassekonzentration, die Biomasseproduktivität, die Wachstumsrate und den Ertrag zu maximieren. Nachdem die Glukosekonzentration für *Chlorella vulgaris* optimiert wurde, konnte eine Steigerung der Biomassekonzentration von 6 % und eine Steigerung der Wachstumsrate um 60 % beobachtet

werden. Zusätzlich dazu haben sich der Ertrag und die Biomasseproduktivität beinahe verdreifacht. Bei *Schizochytrium mangrovei* konnte die Biomassekonzentration um 12 % erhöht und eine zehnfach höhere Wachstumsrate erreicht werden, nachdem die Nährstoffkonzentrationen optimiert wurden. Die Biomasseproduktivität hat sich verzehnfacht und der Ertrag fast vervierfacht. In Batchfermentationen von *Chlorella vulgaris* wurde eine hohe Sensibilität der Zellen auf die vom Rührer verursachten Scherkräfte beobachtet. Aufgrund schlechter Sauerstoffsättigungsregulationen wurden in den Fermentern geringere Produktivitätskennzahlen als in den Kolbenversuchen erzielt. Die Batchfermentationen von *Schizochytrium mangrovei* resultierten in einer Nährstofflimitierung aufgrund der Hitzesterilisation des Mediums, was durch Airflift-Bioreaktor Versuche bestätigt wurde. Die Analyse des *Schizochytrium mangrovei* Lipids deckte einen Lipidgehalt von 45 % auf, mit einem hohen Prozentanteil von Docosahexaensäure (DHA). Die Resultate aus den durchgeführten Experimenten zeigten, dass die heterotrophe Kultivierung der zwei Mikroalgen ein vielversprechender Ansatz für deren industrielle Nutzung ist. Durch weitere Optimierung können die Produktivitätskennzahlen noch gesteigert werden.

TABLE OF CONTENT

1. OBJECTIVE AND STRUCTURE OF THE THESIS

The main objective of this master thesis was to study the eukaryotic microbiome of microalgae in different natural habitats. Differences and similarities between the eukaryotic microbiome of various habitats were investigated. Furthermore, the industrial applicability of heterotrophic cultivation of specific microalgae was evaluated. Therefore, two types of microalgae suitable for producing industrially interesting products were studied. For both strains, the key indicators biomass concentration and productivity, growth rate and yield were determined for optimal growth conditions. For *Chlorella vulgaris* the focus for the optimization was set on the biomass itself whereas for *Schizochytrium mangrovei* it was set on the production of poly unsaturated fatty acids (PUFAs).

Structure of this thesis:

Chapter 1 is the current chapter and states the objectives of this thesis.

In **Chapter 2** a general introduction to microalgae and their industrial application is provided. For the two microalgae *Chlorella vulgaris* and *Schizochytrium mangrovei* a comprehensive overview is given.

In **Chapter 3** the materials and methods utilized for the microbiome study and the heterotrophic cultivation experiments are specified.

Chapter 4 states the results of all conducted experiments.

Chapter 5 is the discussion of the results.

In **Chapter 6** the drawn conclusions and an outlook providing ideas for further research are stated.

2. INTRODUCTION

2.1. Microalgae in their natural habitat

Microalgae are photosynthetically active microorganisms. They are able to use sunlight to convert inorganic substances, like carbon dioxide, into complex organic compounds such as carbohydrates, fats and proteins, which are necessary for them to live (Day, Gong & Hu, 2017). They can be classified into two main groups: eukaryotic photoautotrophic organisms and prokaryotic cyanobacteria (also known as blue-green algae). Due to their photosynthetic ability, microalgae are very important for the world´s ecosystem. They represent approximately 50% of the global photosynthetic activity and therefore play an important role in the world´s carbon cycle (Singh & Saxena, 2015).

The natural habitats of microalgae vary greatly with the species. They can be found in freshwater, seawater, highly saline water, soil, sands and snowfields (Singh & Saxena, 2015). Microalgae are not found isolated in nature; they have a microbiome associated to them. Generally, the microbiome can influence many factors such as the growth and development of the host. It has an influence on the energy metabolism and supplies nutrients to the host (Russell, 2014). For example, the human microbiome was shown to allow the absorption of unobtainable nutrients. It also was shown to have an influence on the human immune system (Turnbaugh et al., 2007). For various plant species a distinct microbiota is associated that was shown to increase their metabolic pathway range. With this, the nutrient absorption can be increased and new defense mechanisms can be implemented (Berg et al., 2014).

The microalgal microbiome specifically is known to have an influence on the microalgae´s growth by supplying nutrients necessary for them. There are studies, which state that microalgae are reliant on vitamin B12 for their growth and obtain this molecule by bacteria and cyanobacteria in their microbiome (Stal & Cretoiu, 2016 and Grossman, 2016). Grossmann (2016) showed that the vitamin B12 amount produced by the microorganisms in the microalgae's microbiome is enough to satisfy the amounts needed for the microalgae to grow. Other studies (Terashima et al., 2017) show that the microbiome associated with natural habitats of microalgae differ tremendously depending on the type of habitat, season and location. Regardless, the knowledge about the microbiome associated with microalgae is still unsatisfactory and needs to be explored in more detail. Especially because of the increasing

industrial interest for the microalgae, a detailed analysis of the associated microbiome is required (Graham & Wilcox, 2015).

Information on the microbiome can be gathered with amplicon studies, which usually involve DNA extraction, amplification, sequencing and bioinformatic evaluation of microbiome samples (Aguiar-Pulido, 2016). The experimental design of the amplicon study allows a differentiation of detectable microorganisms. The differentiation is reached by utilizing different marker genes for the DNA amplification, e.g. 16s rRNA only for prokaryotic microorganisms (Sunagawa et al., 2013). The sequencing results can be used to get multiple forms of information, such as the microorganisms surrounding the host (Aguiar-Pulido, 2016) and the identification of new biocatalysts (Thomas, Gilbert & Meyer, 2012).

2.2. Microalgae in the industry

Microalgae have a large biotechnological potential and thus attract much interest industrially. They can be utilized in multiple industry fields for producing compounds for environmental purposes, food supplements, cosmetic supplements and many more applications. Its biomass is used for the production of bioactive compounds, fine chemicals, polysaccharides, lipids, pigments, proteins, vitamins and antioxidants (Table 1) (Khan, Shin & Kim, 2018).

Table 1: List of microalgal products. Product groups are defined by the compounds which are commercialized *(Priyadarshani & Rath, 2012)*.

Product groups	**Specific products**
Pigments/Carotenoids	B-carotene, astaxanthin, lutein, zeaxanthin, canthaxanthin, chlorophyll, phycocyanin, phycoerythrin, fucoxanthin
Polyunsaturated fatty acids (PUFAs)	DHA(C22:6), EPA(C20:5), ARA(C20:4), GAL(C18:3)
Vitamins	B1, B6, B12, C, E, biotin, riboflavin, nicotinic acid, pantothenate, folic acid
Antioxidants	Catalases, polyphenols, superoxide dismutase, tocopherols
Other	Antimicrobial, antifungal, antiviral agents, toxins, amino acids, proteins, sterols, MAAs for light protection

Pulz (2004) estimated the market size for algal products to be US$ 5-6.5 billion per year. From this total US$ 1.25 - 2.5 billion were produced by the food health sector, US$ 1.5 billion were produced by Docosalhexanoic acid (DHA) production and US$ 700 million were generated from agriculture.

As stated by Bitog (2010), microalgal cultivation is done since World War 2. During the war, Germans produced microalgal biomass to use it for food supplementation. The bioreactor systems for the production have been further developed since then, but the production costs are still high. The cultivation of the microalgae can be done in three different ways: photoautotrophically, heterotrophically, or mixotrophically (Chen, Liu & Feng, 2016). For the photoautotrophic growth, the microalgae uses energy from the sunlight to convert inorganic carbon into complex organic substances. For the heterotrophic growth, the microalgae converts organic carbon without the presence of a light source into complex organic compounds. Mixotrophic growth is defined by the ability of the microalgae to use organic as well as inorganic carbon sources in the presence of light to grow (Liu, Sun, & Chun, 2014). Not every microalgae has the ability to grow heterotrophically, so dependent on the microalgae an according cultivation type must be chosen (Chen, Liu & Feng, 2016).

2.2.1. Heterotrophic growth of microalgae

The heterotrophic growth of microalgae describes the ability of single cells to utilize organic carbon sources like glucose for the production of lipids or the respiration system and other metabolic pathways (Figure 1). Different organic carbon sources can be used as a growth substrate for the microalgae, like acetate, alcohols and organic acids. The organic carbon source, which leads to the highest growth rates and respiration, varies for different microalgae. However, glucose is reported to yield the best results for the majority of microalgae (Mohan et al., 2014). The ideal concentration of the organic carbon source also varies with each microalgal species (Liu, Sun & Chun, 2014).

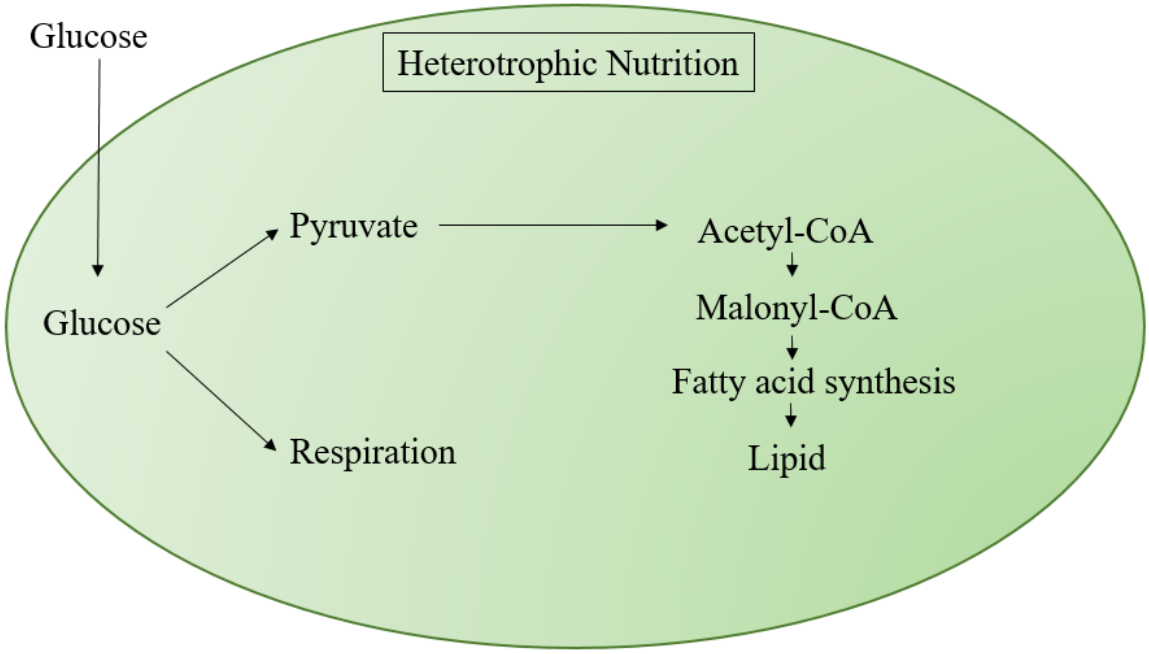

Figure 1: Overview of the heterotrophic nutrition of microalgae. The glucose utilization is shown inside the cell. The glucose entering the cell is either utilized in the respiration and other metabolic pathways or is entering the fatty acid synthesis and converted into lipids. The schematic illustration was constructed according to Mohan et al., 2014.

According to Morales-Sanches (2016), the heterotrophic nutrition mechanism can result in higher biomass concentrations compared to the photoautotrophic mechanism. The reason behind it might be the flux of the pathways used to utilize the carbon source. In the heterotrophic mechanism the pentose phosphate pathway (PPP) is used whereas in the photoautotrophic mechanism the Embden Meyerhoff pathway (EMP) is active. Literature suggests that depending on the carbon source used the flux of the PPP pathway is faster compared to the EMP pathway (Mohan et al., 2014).

Even though the heterotrophic growth is documented to be faster than the photoautotrophic growth, not every microalgae is able to use organic carbon sources to grow. Some microalgae, like multiple *Chlorella sp.*, are documented to grow heterotrophic as well as phototrophic. However, some microalgae are only capable of growing heterotrophically (e.g. Thraustochytrids) or photoautotrophically (Hu et al., 2018).

2.2.2. *Chlorella vulgaris*

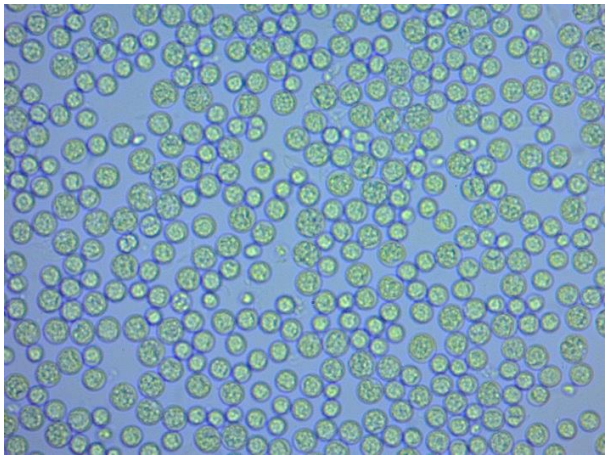

Figure 2: Microcopy picture of *Chlorella vulgaris* . It shows the microalgae with 600x magnification.

Chlorella vulgaris is a unicellular non-mobile green microalgae (Figure 2). It belongs to the family of *Chlorellaceae*. *Chlorella vulgaris* was first described by M. W. Beyernick (1890). The shape of the cells is spherical or ellipsoidal and they have a diameter of 2 to 15 µm. Their natural aqueous habitat includes freshwater, marine water and soil (Chen, Liu & Feng, 2016). The reproduction of *Chlorella vulgaris* occurs asexually through autosporulation (Figure 3). The cell divides itself into multiple daughter cells. The cell wall of the parent cell breaks open and the new *Chlorella vulgaris* cells are released (Safi et al., 2014). A division into up to 16 daughter cells is documented (Beyerinck, 1890).

Chlorella vulgaris is able to grow phototrophically but also heterotrophically which makes it a very interesting organism for fermentation processes. (Chen, Liu, & Feng, 2016).

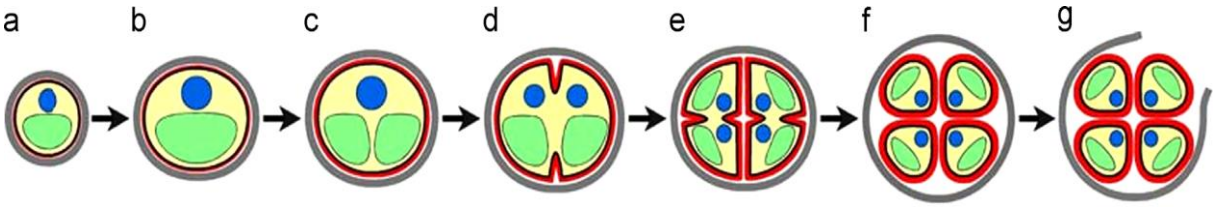

Figure 3: Cell division of *Chlorella vulgaris*. a) initial growth phase; b) late growth phase; c) division of chloroplast; d) early protoplast division; e) late protoplast division; f) daughter cells maturation; g) hatching phase (Safii et al., 2014)

2.2.2.1. Chlorella vulgaris as a commercial product

The biomass of *Chlorella vulgaris* provides a large number of potential products (Chen, Liu & Feng, 2016). A look into the biomass composition of *Chlorella vulgaris* gives an initial idea for the products, which can be produced with this microalgae (Table 2).Worth mentioning here is the high protein content of the microalgae (Priyadarshani & Rath, 2012). The protein profile shows the presence of all the essential amino acid that humans need to take in by food

consumption (Wells et al., 2017), making it an ideal candidate as a food supplement. Also, the high lipid content, which can be largely influenced by using different media, makes the microalgae an interesting object for industrial purposes for the production of biodiesel (Shen et al., 2015).

Table 2*: Chlorella vulgaris´* composition of dry biomass *(Priyadarshani & Rath, 2012)*. The table includes the protein, carbohydrate and lipid content in percent.

Microalgae	Protein (%)	Carbohydrate (%)	Lipid (%)
Chlorella vulgaris	41-58	12-17	10-22

Especially the presence of Vitamin B12 in the biomass of the microalgae is notable. Vitamin B12 is very important for many metabolic processes of humans (Kumusha et al., 2010) and is therefore often supplemented into food products. *Chlorella vulgaris* is rich in pigments like chlorophyll and beta-carotenes, which have antioxidant effects. They are also protective against degeneration processes of the retina and have a regulatory influence on the blood cholesterol. For these reasons, they are desired as food supplement products (Safi et al., 2014).

Currently, the dry biomass of *Chlorella vulgaris* is sold as food additive for improvement of the protein and nutritional content. They can be found in smoothies, salad dressings, beverages and other products (Wells et al., 2017).

2.2.3. *Schizochytrium mangrovei*

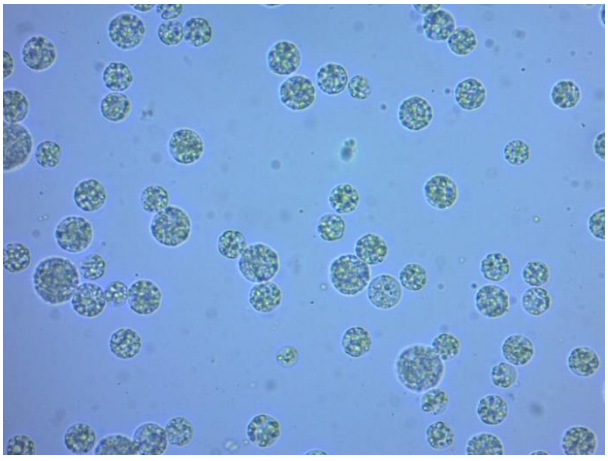

Figure 4: Microscopy picture of *Schizochytrium mangrovei* . It shows the microalgae with 600x magnification.

Schizochytrium mangrovei (Figure 4) is part of the *Thraustochytrida* order. Thraustochytrids are not a classical microalgae, they lack any sort of photosynthetic apparatus, are therefore incapable of photosynthesis and grow strictly heterotrophic (Leyland, Leu & Boussiba, 2017).

Natural habitats of this microalgae include saline waters and sediments as well as the surface of marine plants (Dayal, 1996).

The life cycle of *Schizochytrium mangrovei* consists of 3 main steps which can be seen in Figure 5 (Hong, Nhat, & Ahn, 2016):

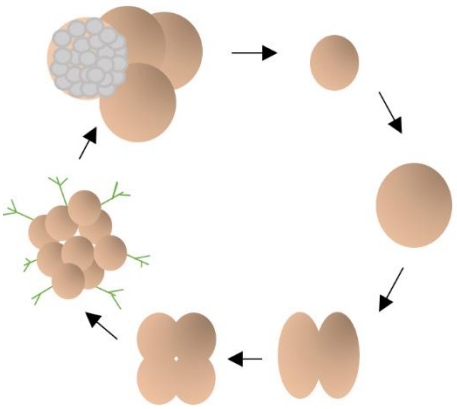

1. Zoospores of the microalgae will round up and form mobile amoeboids.
2. The amoeboids will lose their mobility and grow by cell division. The microalgae tends to cluster together during their growth.
3. The fully grown cell will release mobile spores and the cycle will be repeated.

Figure 5: Lifecycle of *Schizochytrium mangrovei* . The lifecycle of the microalgae consists of 3 main steps. Zoospores form mobile cells which will lose their mobility and grow by cell division until the cell releases again zoospores. The schematic illustration was constructed according to Benne et al., 2017.

2.2.3.1. Schizochytrium mangrovei as a commercial product

The Thraustochytrids are widely utilized as a source for omega-3- and omega-6-fatty acids (Leyland, Leu & Boussiba, 2017). Especially *Schizochytrium mangrovei* is known for its very high lipid content of 50-77% w/w (Priyadarshani & Rath, 2012). The lipid profile of the microalgae reveals a high content of the omega-3-fatty acid DHA (30-50% w/w), varying depending on the microalgal strain and cultivation medium used (Chodchoey & Verduyn, 2012 and Sahin, Tas & Altindag, 2018).

The high lipid content of *Schizochytrium mangrovei* makes it an ideal candidate for biodiesel production (Gupta et al., 2016). The ability of *Schizochytrium mangrovei* to produce DHA makes it a very interesting microorganism for the food and pharmaceutical industry (Priyadarshani & Rath, 2012). DHA is a long chain poly unsaturated fatty acid (LC-PUFA). LC-PUFAs do have a positive influence on the human health (Mühlroth et al., 2013). New studies suggest LC-PUFAs have the potential to aid in the treatment of neurological and –degenerative illnesses and have shown protective effects on the human brain (Dyall S. C., 2015). DHA and EPA are sold as food additives to improve the nutritional value of the food product and as dietary supplements (Priyadarshani & Rath, 2012).

2.2.3.1.1. Docosahexaenoic acid (DHA) & eicosapentaenoic acid (EPA) synthesis

The synthesis process of DHA and EPA can be seen in Figure 6. DHA is an elongation product of EPA, therefore they share the majority of the pathway. The precursor for these longer chain PUFAs is alpha linolenic acid (ALA). In the first step ALA is desaturated. This initial step is rate limiting. Next is an elongation step followed by a second desaturation step which is catalyzed by the enzyme Δ5 – desaturase. The second desaturation step produces EPA. All the mentioned steps take place in the endoplasmic reticulum. Further elongations of EPA and a location change to the peroxisome than lead to the production of DHA. The enzyme(s) responsible for the elongation steps is not known (Dyall & Michael-Titus, 2008).

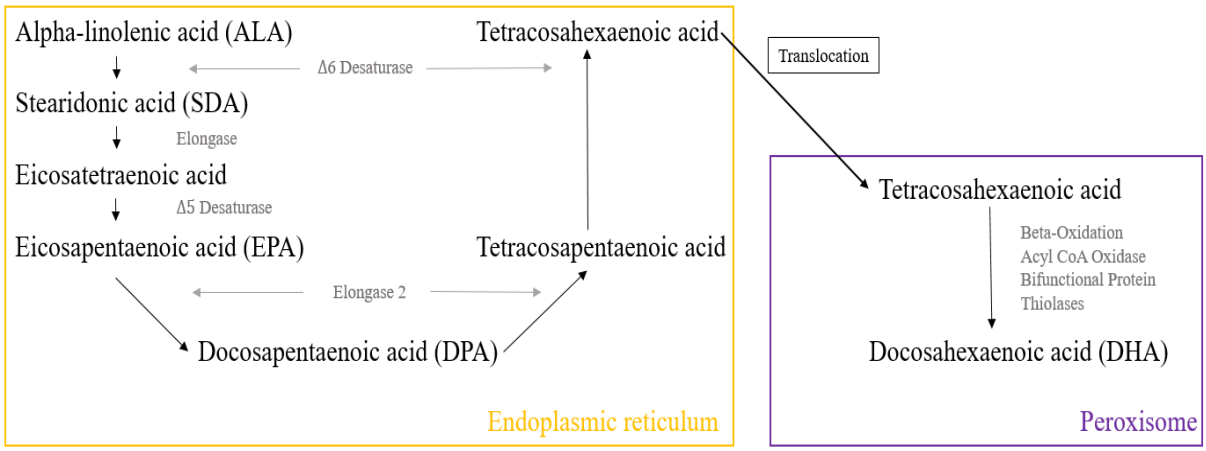

Figure 6: Pathway for the synthesis of LC- PUFAs docosahexaenoic acid (DHA) and eicosapentaenoic acid (EPA) from alpha linolenic acid (ALA). The synthesis consists of multiple elongation and desaturation steps. DHA is an elongation product of EPA. The schematic illustration was constructed according to Dyall, 2015.

3. MATERIAL & METHODS

3.1. Amplicon study

3.1.1. Sampling

Samples from 44 habitats were collected from different geographic locations in Austria (Figure 7): Triebener Tauern, Drei Lacken, Seetaler Alpen, Graz and Ennstal. They were taken from different (micro-)habitats at different altitudes: lakes, stagnant waters, snowfield, a plastic chair and tiles from a pool. From each location multiple replicates were obtained (Table 3).

Figure 7: Origin of the amplicon study samples. Representative pictures of the locations of the samples used in the amplicon study can be seen. Samples were taken from 5 different locations (Triebener Tauern, Drei Lacken, Seetaler Alpen, Graz, Ennstal) and habitats (snowfield, lake, water, chair, tile).

Table 3: Amplicon sample description including the names used further in the thesis, replicates taken, location of the samples as well as the habitat.

Name	Replicate	Location	Habitat
1A	a,b,c,d,e,f,g	Triebener Tauern	red snowfield
1B	a,b,c,d,e,f,g		green snowfield
2A	a,b	Drei Lacken	Pond
2B	a,b		Pond
2C	A		swimming pond
3A	a.b.c	Seetaler Alpen	red snowfield
3B	a,b,c		stagnant water
3C	b,c		lake
3D	a,b,c,d,e		orange snowfield
3E	a,b,c		red snowfield
chair	Garten1, Garten2, Garten3	Graz	red biofilm
pool	Pool1, Pool2, Pool3, Pool4, Pool5, Pool6	Ennstal	tile of a pool

3.1.2. DNA extraction

For each sample 2 mL of algae suspension were centrifuged at 13,000 rpm for 20 minutes at 4 °C. The supernatant was discarded and the pellets were used for DNA extraction using FastDNA SPIN kit for soil (MP Biomedicals, Eschenberg, Germany) according to manufacturer's protocol. Briefly, 978 µL sodium phosphate buffer and 122 µL MT buffer were added to respective pellets. For mechanical lysis, the cells were homogenized in a FastPrep FP120 instrument for 30 seconds at a speed of 5.5 m s^{-1}. After 15 minutes centrifugation at 14,000 × g, 250 µL protein precipitation solution (PPS) was added to the supernatant. After another five minutes centrifugation (14,000 × g), one mL binding matrix solution was added to the supernatant. After inverting the tube for two minutes by hand the tubes were placed in a rack for ten minutes to allow settling of silica matrix. Approximately 800 µL supernatant were discarded. Resuspended binding matrix was transferred to a spin filter with subsequent centrifugation at 14,000 × g for one minute. After resuspending the pellet in 500 µL SEWS-M the suspension was again centrifuged (14,000 × g, one minute). The catch tube was discarded and replaced by a new, clean catch tube. After air drying in the spin filter for five minutes the binding matrix was resuspended in 56 µL ultrapure water. For better binding, the matrix was incubated for five minutes at 55 °C. After another centrifugation step (14,000 × g, one minute), DNA was ready for further processing and stored at -20 °C until further use. The extracted DNA

of the 44 samples was utilized as a template for PCR amplification. The deployed primers are specifically designed to target the 18S rRNA region of eukaryotic DNA (Table 4).

Table 4: Primers used in for the 18S rRNA amplification including the sequences and the specific primer names.

Primer	Name	Sequence 5´-3´
Forward	Euk 1391f primer-pad	TATGGTAATTGTGTACACACCGCCCGTC
Reverse	EukBr primer-pad	AGTCAGCCAGGGTGATCCTTCTGCAGGTTCACCTAC

The first step in preparing the samples for sequencing was to increase the DNA concentration of the target DNA. Therefore, two different types of PCRs were conducted.

3.1.3. Amplification of 18S rRNA gene fragments for Illumina sequencing

All DNA samples have been used for a PCR, where the primers from table 4 were utilized. The temperature program for this PCR is described in Table 5. After the PCR a control gel was performed to confirm the presence of the desired DNA product. With all gels a negative control, nuclease free water, was included. If the gel showed a band for a sample, this sample was ready for further processing. If no band was detected a nested PCR was performed with the respective samples.

Table 5: Temperature profile for 3.1.1. PCR including the cycle time and repetitions of each step.

Temperature	time	
98°C	5 min	
98°C	10 sec	10x
53°C	30 sec	
72°C	30 sec	
98°C	10 sec	20x
48°C	30 sec	
72°C	30 sec	
72°C	10 min	
15°C	∞	

12 samples did not show a respective band on the gel after the first PCR approach (3Ba, 3Bb, 3Bc, 3Cb, 3Cc, Pool2, Pool4, 1Aa, 2Aa, 2Ab, 2Ba, 2Bb). A nested PCR was necessary to amplify the DNA. For the nested PCR, 2 PCR runs had to be done. The first run results in a

pre-fragment. For this run different primers and a different temperature program were necessary (Table 6, Table7). The second PCR run had the sample protocol. With this run the desired DNA product was amplified.

Table 6: Primers used for 1st nested PCR including sequences and primer names.

Primer	**Name**	**Sequence 5´-3´**
Forward	NS1	GTAGTCATATGCCTTGTCTC
Reverse	NS8	TCCGCAGGTTCACCTACGGA

Table 7: Temperature profile for 1st nested PCR including the time and repetitions of each step.

temperature	**time**	
95°C	10 min	
94°C	1 min	40x
50°C	2 min	
70°C	3 min	
72°C	7 min	
15°C	∞	

After the second PCR a control gel was performed to affirm the existence of the DNA product at the desired height. A positive and negative control were included. The negative control was nuclease free water and the positive control was a sample that verified the correct DNA product after the first PCR approach (Pool1).

After the DNA was amplified to reach a high enough DNA concentration, another PCR was performed for attaching barcode sequences on the target DNA to ensure a correct identification after sequencing. For this, PCR specific barcode primers for each sample were deployed. GOLAY barcode primers were used. The program used for the barcode PCR can be found in Table 8.

Table 8: Temperature profile for barcode PCR including the time and repetitions of each step.

temperature	time	
95°C	2 min	
95°C	30 sec	20x
56°C	30 sec	
72°C	30 sec	
72°C	10 min	
15°C	∞	

A control gel was performed to ensure that all the PCR products were present. A negative control, nuclease free water, was included in the gel. The PCR products were then purified by using the Wizard® SV Gel and PCR Clean-Up System. After measuring the DNA concentration of the barcoded samples using a UV-Vis spectrophotometer (NanoDrop, Thermo Fisher Scientific, Massachusetts, USA) the samples were pooled equimolarly and sent for HiSeq Illumina sequencing (GATC Biotech, Germany).

3.1.4. Bioinformatics and statistical analyses

Joining forward and reverse read pairs was done using the software package QIIME 1.9.1. (Caporaso et al., 2010). After removing barcodes, primer and adapter sequences, reads as well as metadata were imported to QIIME 2 (2017.12 release). The DADA2 algorithm (Callahan, et al., 2016) was used to demultiplex, denoise and truncate reads in order to generate ribosomal sequence variants (RSVs), which were then summarized in a feature table. Chimeras were identified by using the VSEARCH uchime_denovo method (Rognes et al., 2016) and subsequently removed. Phylogenetic metrics were constructed by aligning representative sequences using the mafft program. After the multiple sequence alignment was masked and filtered a phylogenetic tree was generated with FastTree. The taxonomic analysis was based on a customized naïve-bayes classifier trained on 18S rRNA gene OTUs clustered at 99% similarities with the SILVA128 database release and trimmed to a length of 200 bp. The dataset was normalized to 11,000 reads per sample to account a variation in the samples. Feature table was reduced by retaining only features with an absolute abundance of more than 100 overall samples. Normalized feature tables served as input for following alpha and beta diversity analyses using QIIME 2 core diversity metrics. Principal Coordinate Analysis (PCoA) plots were constructed by calculating the unweighted UniFrac distance matrix (Lozupone & Knight, 2005).

3.2. Microalgal strains

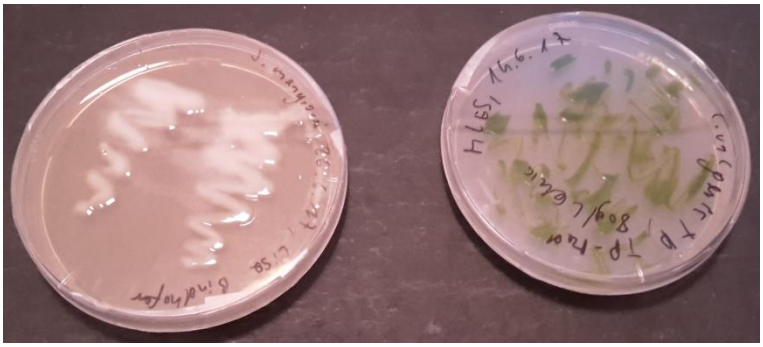

Figure 8: Plate culture of the two microalgal strains used in the thesis. On the left: *Schizochytrium mangrovei* (white slimy culture), on the right: *Chlorella vulgaris* (green culture)

3.2.1. Chlorella vulgaris

The BEIJ *Chlorella vulgaris* production strain, 1996/H 14 Doucha et Livansky strain (Pat.N. 299352) used in this work was provided by the Institute of Microbiology, CAS, Centre Algatech (Trebon, Czech Republic)

3.2.1.1. Strain maintainance

Chlorella vulgaris was kept on agar plates to maintain the microalgae viable as seen in Figure 8. The culture was transferred to a new plate each month to ensure the microalgae's survival. 25 ml of a liquid culture were cultivated in a 25cm^3 CELLSTAR® Filter Cap Cell Culture Flask by Greiner Bio One at all times. New flasks were inoculated every two weeks.

3.2.2. Schizocyhtrium mangrovei

Schizochytrium mangrovei CKM1 also known as *Aurantiochytrium mangrovei* CKM1 was used in this master thesis. The microalgae was supplied by the project partner BioEnergy2020+ (Tulln, Austria).

3.2.2.1. Strain maintenance

Yeast extract – peptone – dextrose (YEPD) plates were used for the cultivation of *Schizochytrium mangrovei* as seen in Figure 8. The plates were restreaked every other week. 25 ml of liquid culture were constantly kept in a 25cm^3 CELLSTAR® Filter Cap Cell Culture Flasks by Greiner Bio One. The 25cm^3 flasks were renewed weekly.

3.3. Medium

3.3.1. Chlorella vulgaris

For the cultivation medium of *Chlorella vulgaris*, 5 different stock solutions (stock solution 1, 2, 3, 4, 5) and one base solution were prepared. All solutions were autoclaved at 121 °C for 15 min (autoclave Systec V-150), except the stock solution 2. This stock solution needed to be sterile filtered. Therefore, a pre-autoclaved 1L glass bottle was needed. The autoclaved glass bottle was attached to a filter unit. A 0.2µm filter from sartorium sterdim biotech was used to sterile filter the stock solution 2. All sterile stock solutions were stored at 4°C. Specific amounts of volumes of the stock solutions were added to the base solution to create the cultivation medium. A pH of 7.5 was set by using 1M NaOH or 1M HCl.

The glucose used for the experiments was autoclaved separately. A glucose stock solution was prepared (300 g L^{-1}) and stored at room temperature.

The composition of the medium used for the cultivation of *Chlorella vulgaris* is described in the internal standard operating procedure "Chlorella_vulgaris_medium" of BDI – BioEnergy International GmbH (Graz, Austria).

For the agar plate cultivation of *Chlorella vulgaris* the same medium was used adding 15 g of agar-agar before the autoclaving to the base solution to solidify the medium. The pH of the medium was adjusted to 6.2. The stock solutions and 80 g L^{-1} glucose were added after the agar-agar solution was cold enough. The plates were poured inside of a Laminar Flow (Hera Safe, Thermo Scientific) to ensure sterility. Once the plates solidified they were stored at 4 °C.

3.3.2. Schizochytrium mangrovei

3.3.2.1. Liquid medium

The medium utilized for the liquid cultivation of *Schizochytrium mangrovei* consisted of the components listed in Table 9, Table 10 and Table 11.

Table 9: Composition of 1L ASW medium *(Rappel, 2013)* MOPS puffer was not used for the fermentation.

Component	**Conc. Stock Solution [g L^{-1}]**	**Amount**	**Unit**
NaCl	-	25.00	g
$MgCl_2$ * 6 H_2O	-	2.00	g
KCl	-	0.50	g
$NaNO_3$	-	0.75	g
$MgSO_4$ * 7 H_2O	-	3.50	g
$CaCl_2$ * 2 H_2O	-	0.50	g
MOPS-Puffer	-	42.00	g
Citric acid monohydrate stock	3.28	1.00	mL
Ferric ammonium citrate stock	3.00	1.00	mL
Na_2EDTA * 2 H_2O stock	0.5025	1.30	mL
Na_2CO_3 stock	20.0	1.00	mL
Spurenelemente stock	Table 10	1.00	mL
After heat sterilization the following components are added			
K_2HPO_4	57.265	1.00	mL
Vitamin Stock	Table 11	1.00	mL

Table 10: Composition of 1L of trace element stock solution *(Rappel, 2013)*

Trace Element	**M [g mol^{-1}]**	**amount [g]**	**Conc. [mM]**
H_3BO_3	61.83	2.860	46.25
$MnCl_2$ * 4 H_2O	197.91	1.810	9.15
$ZnSO_4$ * 7 H_2O	287.56	0.222	0.77
Na_2MoO_4 * 2 H_2O	241.95	0.390	1.61

$CuSO_4 * 5 H_2O$	249.69	0.079	0.32
$CoCl_2 * 6 H_2O$	237.93	0.040	0.17

Table 11: Composition of 1L of vitamin stock solution *(Rappel, 2013)*

Component	Amount	Unit
Vitamin B12	0.1352	g
Biotin	0.0250	g
Thiamin HCl	1.0960	g

As a nitrogen source 0,03M Urea and 0,03M $(NH_4)_2SO_4$ were tested. Therefore, a 1 M Urea and 1M $(NH_4)_2SO_4$ stock solution were made, sterile filtered and stored at 4°C.

All the individual parts of the medium were sterile filtered as well. The medium consists of 50 % ASW (Table 9, Table 10, Table 11), 0,03M of a nitrogen source, glucose and deionized water.

For the glucose, a stock solution was prepared (300 g L^{-1}) and heat sterilized at 121°C for 15 min.

3.3.2.2. Solid medium

The solid medium used for *Schizochytrium mangrovei* was a simple YEPD medium that additionally contained salts. The composition of the solid medium can be seen in Table 12.

Table 12: Composition of 1L YEPD medium including artificial seasalt (ASS)

Component	Amount [g]
Pepton	20
Yeast extract	10
Glucose	20
Agar	15
$MgSO_4$	0.602
NaCl	0.467
$MnCl*4H_2O$	0.001

All compounds except for glucose were dissolved in 1L water. The liquid was sterilized (15 min, 121°C, autoclave). The glucose was added, once the liquid was cool enough. The plates were poured in a Laminar Flow.

3.4. Flask experiments

To determine the optimal substrate concentration for each microalgae, flask experiments were conducted. In addition to the ideal substrate concentration, for *Schizochytrium mangrovei* two different nitrogen sources, Urea and $(NH_4)_2SO_4$, were tested.

3.4.1. Substrate concentration

For these experiments, 300 ml pre-autoclaved flasks with baffles were utilized. The flasks were closed with sponge flask caps. The preparation of the flasks was performed in a Laminar Flow (Hera Safe, Thermo Scientific) to affirm sterility of the medium as well as the culture. 100 mL of medium were placed into the pre-autoclaved flasks for the cultivation. Depending on what glucose concentration was needed in the flask, different volumes of the glucose stock solution were added to the medium by using single-use serological pipettes. An inoculum of 5% (v/v) was used for each flask. The inoculum was provided by the 25cm^3 CELLSTAR® Filter Cap Cell Culture Flasks by Greiner Bio One. Here, a single-use serological pipette was used as well to avoid any contamination of the culture. After the inoculation, the flasks were kept in a shaking unit (Infors Ht Multitron) with a shaking frequency of 130 rpm. *Chlorella vulgari*s was cultivated at 35 °C and *Schizochytrium mangrovei* at 28 °C. Daily samples were taken in a Laminar Flow. The samples underwent several measurements (3.7. cultivation data analysis). The pH value and the temperature of the flasks were measured to monitor the condition of the liquid culture. A microscopy was performed looking for any contamination and to observe the state of development of the cells.

For *Chlorella vulgaris* substrate concentrations ranging from 40 – 80 g L^{-1} glucose were tested, whereas for *Schizochytrium mangrovei* 40 – 120 g L^{-1} glucose concentrations were tested.

3.4.2. Nitrogen source

For *Schizochytrium mangrovei* two different nitrogen sources were tested: 30 mM Urea and 30mM $(NH_4)_2SO_4$. Instead of changing the substrate concentration, the nitrogen source was changed. The substrate concentration chosen for these experiments was 40 g L^{-1} glucose to avoid substrate inhibition. The flask preparation was performed in a Laminar Flow. All medium components were transferred into the pre-autoclaved flask. Depending on what nitrogen source

used, 30 mM of the right solution (either Urea or $(NH_4)_2SO_4$) was added. The handling of the flasks was exactly the same as described in 3.4.1. Substrate concentration.

3.5. Batch fermentation

Once the ideal substrate and nitrogen concentrations were identified, multiple batch fermentations were performed. The fermenter used was an Infors HT Techfors-S with a working volume of 5 L (Figure 9). The temperature was regulated through a double coat. Sterile air was provided through an air filter at the air inlet. The same filter was used at the air outlet. The air entered the vessel via a sparger, which was located underneath the Rushton impeller stirrer. Acid (2 M HCl), base (2 M NaOH) and an antifoaming agent (Glanapon2000) were supplied by a pumping system. A foam detector, located on top of the fermenter vessel, measured the foam in the fermenter. Antifoaming agent was added accordingly. A pH and pO_2 probe measured the pH value and oxygen saturation inside the vessel continuously. A small computer with touchscreen, located directly next to the fermenter as part of the regulatory unit, allowed controlling of the fermentation process. Additionally, the computer program IRIS was utilized for controlling and documenting the fermentation process.

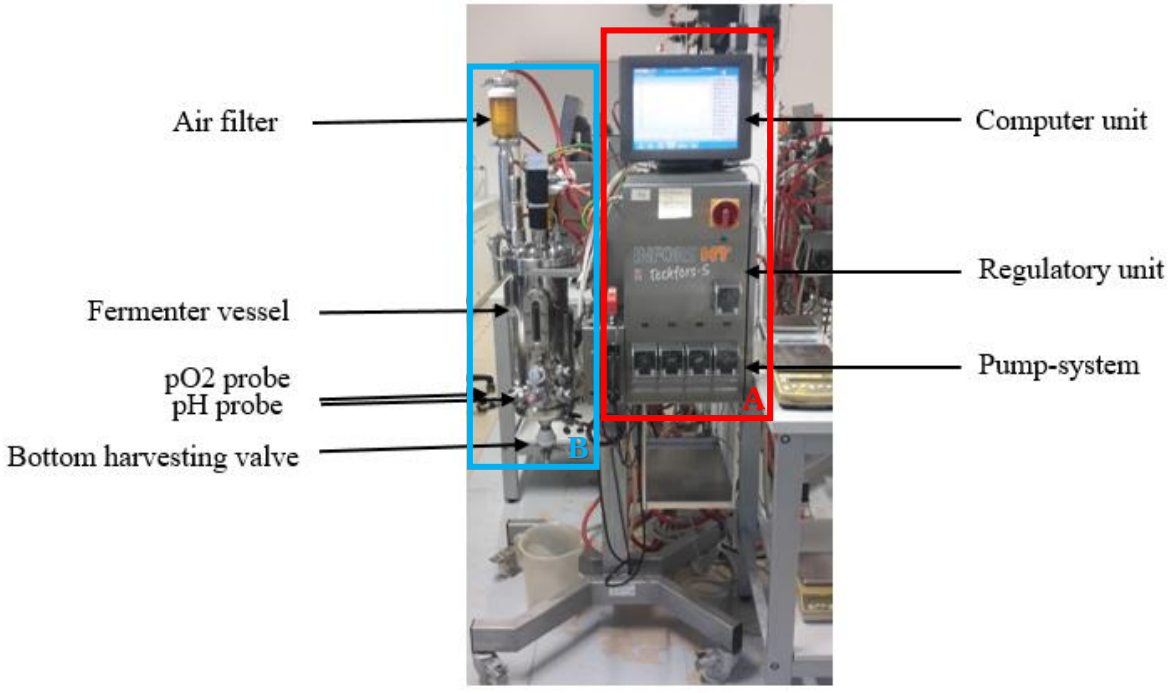

Figure 9: Infors HT Techfors-S fermenter used for the batch experiments. The fermenter included a regulatory system (A) next to the fermenter vessel (B).

For the batch fermentation the fermenter was prepared as follows: The fermenter was prewashed with hot water and filled up with medium. The trace element solution, vitamin solution and glucose were not added into the medium. The trace elements and vitamins are not able to handle high temperatures and the addition of glucose would lead to the maillard reaction and an associated loss of nutrients. For the sterilization process all openings of the fermenter were closed. In situ sterilization with hot steam was performed with a holding time of 30 min at a temperature of 121 °C. Parallelly, the acid, the base, the antifoam agent, the glucose flask filled with glucose and the empty inoculation flask were autoclaved.

Once the sterilization and autoclaving process were completed, the acid, base and antifoam agent were added to the fermenter. To ensure sterility at this step, the septum was covered with ethanol (70%) and flamed. The needle of each flask was stung through the burning septum and bolted securely. Next, the settings for the fermentation process were set with the computer program IRIS. Before inoculation, the trace elements were provided by using a sterile filter on a syringe. The septum was covered with ethanol (70%) to ensure sterility whilst the syringe was stuck through it.

Afterwards, when fermentation parameters became constant, the fermenter was ready for inoculation. The culture used was examined by microscopy. The sample for this was taken under the Laminar Flow. The OD of the culture was measured at a wavelength of 750 nm. The measured OD_{750} was then utilized for calculating the required volume to start the fermentation process with a starting OD_{750} of 1. The inoculum was then transferred into the inoculation flask under the Laminar Flow. Shortly before the inoculation, the process documentation by the program IRIS was started. For the inoculation the septum was covered with ethanol (70%) and flamed.

Daily samples were taken from the valve at the bottom of the fermenter. To keep the fermenter sterile, the valve was flooded with steam before and after sampling. The OD_{750} and the glucose concentration were measured as described in 3.7. Cultivation data analysis. The biomass concentration was measured differently due to the bigger volume available. It was calculated as described in 3.7. Cultivation data analysis.

Once the glucose was used up the fermentation was stopped. The fermentation broth was harvested through a valve at the bottom of the fermenter vessel. After usage, the fermenter was cleaned with hot water. The fermentation broth was further analyzed.

In Table 13 the starting parameters for the fermentation of *Chlorella vulgaris* and *Schizochytrium mangrovei* are summed up. Three fermentations were performed for each microalgae. In each step the pO_2 regulation cascade was adjusted. The different regulations cascades can be found in Table 14.

Table 13: Starting set points for the batch fermentations of *Chlorella vulgaris* and *Schizochytrium mangrovei* including temperature [°C], pH value, glucose concentration [g L^{-1}], stirrer speed [rpm], airflow [NL/min], pO_2 [%]

	Chlorella vulgaris	***Schizochytrium mangrovei***
Temperature [°C]	35	28
pH value	7.5	7
Glucose concentration [g L^{-1}]	40	40
Stirrer [rpm]	100	100
Airflow [NL min^{-1}]	2	2
pO_2 [%]	80	80

Table 14: pO_2 regulation cascades for each performed batch fermentation. The table shows the adjusted pO_2 regulation cascades to optimize the batch fermentation of each microalgae.

Fermentation	**pO_2 regulation cascade**
	Chlorella vulgaris
1	stirrer [100-1500 rpm] – flow [2-10 NL min^{-1}] – pressure [0-1 bar]
2	flow [2-10 NL min^{-1}] – pressure [0-1 bar] – stirrer [100-500 rpm]
3	flow [2-10 NL min^{-1}] – pressure [0-1.5 bar] – stirrer [100-500 rpm]
	Schizochytrium mangrovei
4	Flow (max. 10 NL min^{-1}) – Gas mix (max. 50 %) – pressure (max. 1 bar); stirrer constant
5	Flow (max. 10 NL/min) – Gas mix (max. 50 %) – pressure (max. 1 bar); stirrer constant
6	Stirrer (max. 600 rpm) – Gas mix (max. 50 %) – pressure (max. 1.5 bar); airflow constant

3.6. Airlift bioreactor

Due to apparent growth inhibition of *Schizochytrium mangrovei* in the fermenter, further cultivation experiments in a 5 L airlift bioreactor were conducted.

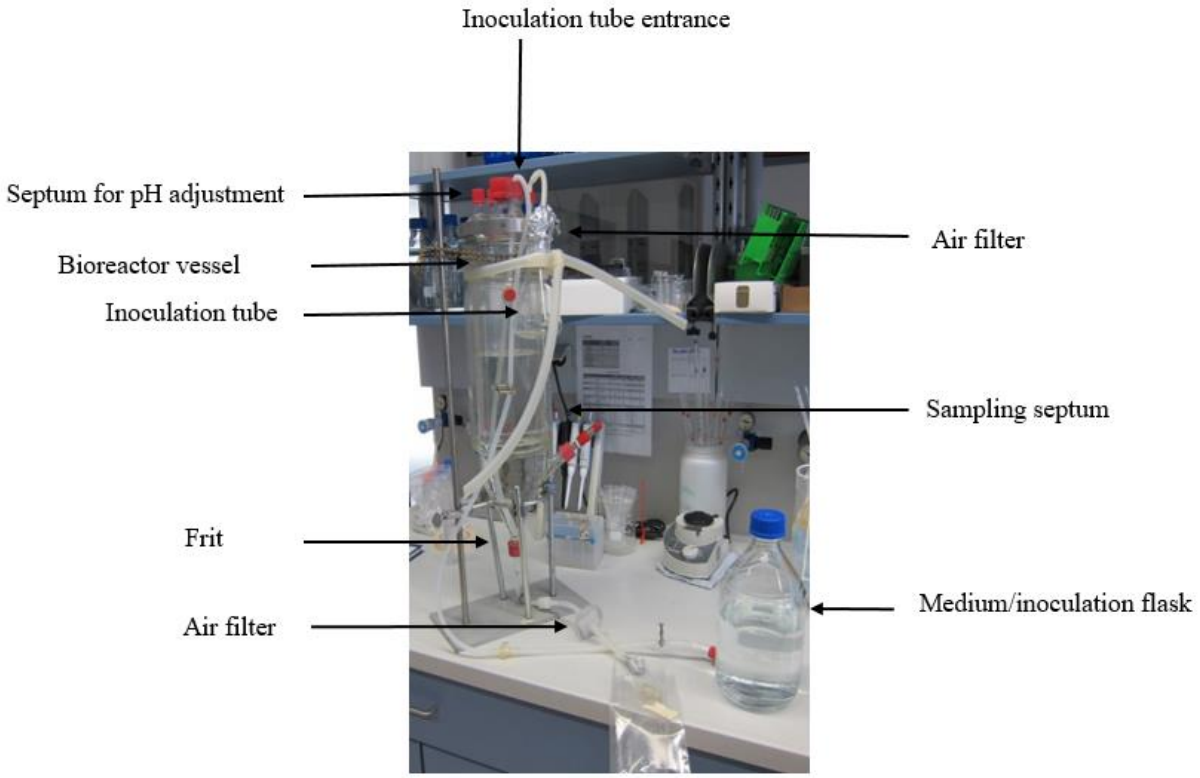

Figure 10: Airlift bioreactor used for cultivation experiments . The parts used for the construct are labeled in the figure.

The utilized bioreactor can be seen in **Figure *10***. A frit at the bottom supplied air to the vessel. The air was sterile filtered before entering the system. A pH probe was installed for continuous measurement. The probe needed to be submerged into liquid at all times, therefore, the vessel was filled with 1 liter of medium or water, depending on the experiment conducted. At the top of the vessel a tube was placed for inoculation purposes and medium fulfillment. The tube was long enough to be submerged into the liquid inside the bioreactor on one end and on the other end the tube was attached to a 2 L glass bottle (medium/inoculation flask). Additionally, one opening was plugged with a septum for pH adjustment. On the side of the fermenter an opening was provided with a septum for sampling.

For sterilization the system was placed into the autoclave. After sterilization the pH probe was activated and the trace element solution was added through the side septum. All septum were covered with Ethanol (70%) before usage. To establish the correct pH value, 2 M HCl and 2 M NaOH were utilized in a syringe with a single-use cannula at the top septum. Next, the missing

medium component (either glucose or ASW+glucose) was added by using the medium/inoculation flask. Once all the components of the medium were inside the bioreactor, the medium/inoculation flask was placed under the Laminar Flow, the inoculum was transferred into the flask and then in the bioreactor. Before using the inoculum, the culture was examined microscopically. The sample for this was taken under the Laminar Flow. The OD of the culture was measured at a wavelength of 750 nm. The measured OD_{750} was then utilized for calculating the required volume to start the cultivation process with a starting OD_{750} of 1. After inoculation the tube was closed with a hose clamp. If necessary, the pH was adjusted throughout the cultivation period by manually adding the base or acid. Daily samples were taken and examined the same way as the fermenter samples have been (see 3.7. Cultivation data analysis).

3.6.1. Fermentation simulation

For the fermentation simulation experiment the bioreactor was autoclaved twice for simulating the 121 °C for 30 min sterilization of the fermenter. During autoclaving all medium components except for glucose and trace element solution were inside the bioreactor, which was the same situation for the fermentation. The glucose solution was located in the inoculation flask and autoclaved with the bioreactor, similar to the fermentation.

3.6.2. Filtered medium cultivation

For the filtered medium cultivation the bioreactor was filled only with 1L water during autoclaving to submerge the pH probe. After the sterilization process of the cultivation equipment, the media flask, still attached to the inoculation tube, was placed into the Laminar Flow, filled up with the sterile filtered medium and glucose and added to the bioreactor. The same was done with the inoculum. For this cultivation, additionally to the air supply an oxygen tank was attached to the air supply to increase the oxygen inside the bioreactor. The additional oxygen supply was regulated manually.

3.7. Cultivation data analysis

The data generated from the cultivation experiments (flask experiments, fermentation, bioreactor cultivations) were analyzed with Excel. The values calculated were used to evaluate the cultivation processes and to compare the different experiments.

3.7.1. Dinitrosalicylic acid (DNS) – assay

The glucose concentration in the culture medium was measured with the DNS – assay. The reaction principle behind it can be seen in Figure 11. If the 3,5-dinitro-salycilic acid reacts in an alkaline environment with a reducing sugar like glucose, it gets reduced to 3-amino-5-dinitrosalycilic acid. This product has an orange color and the intensity of the color is dependent on the amount of reducing sugar present (Toledo et al., 2012).

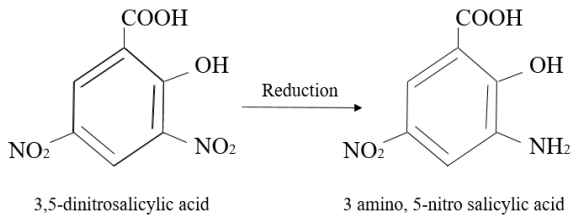

Figure 11: Reaction scheme of DNS and a reducing sugar. 3,5 dinitro-salycilic acid and the aldehyde group of a reducing sugar react under alkine conditions. 3-amino-5-dinitro salycilic acid is produced which has an orange color.

For the DNS solution 140 mL deionized H_2O (dH_2O) were transferred into a beaker. With a magnetic stirrer system continuous mixing was achieved. 2.5 g Dinitrosalicylic acid were put into the water. Once it is completely dissolved 4.0 g NaOH are added. Next, 75 g of Potassium Sodium tartrate are added over a time period of 20 min. Once there were no solid particles visible, the solution was transferred into a 250 mL glass bottle and filled up with dH_2O. The solution was stored at 4 °C.

The assay was calibrated for a concentration of 1-25 mM glucose. 10 glucose solutions with different concentrations in the mentioned range were created. The samples were further handled like the samples with unknown glucose concentrations. Once the absorptions were known the concentration was plotted against the absorption. Linear regression yielded an equation with a slope *s* and an intercept *i*:

$$Absorption = s * c_n + i$$

This equation can then be used for the calculation of the glucose concentration c_n in the samples.

For the assay a sample from the culture of about 1 mL was taken. The supernatant was gained by using a centrifuge (10,000 rpm, 5 min). If a glucose concentration of over 25 mM was suspected (*e.g.* at the beginning of the cultivation) the supernatant needed to be diluted accordingly. 1 mL of the sample was mixed together with 1 mL of DNS solution in a glass tube. The closed tube was incubated for 5 min at 100 °C in a heating block or water bath. The next step was to cool the tube with ice. Once the sample was cold, 8 mL of dH_2O were added. Then

the sample was measured with a photometer (SpectraMax Plus 384, Molecular Devices) at a wavelength of 540 nm. Each sample was measured 3 times.

For the calculation, the average of the absorption values was calculated. The molar glucose concentration c_n [mM L^{-1}] was calculated with:

$$c_n = \frac{Absorption}{s} - \frac{i}{s}.$$

The molar concentration can then easily be converted to the glucose mass concentration cm [g L^{-1}] with:

$$c_m = \frac{MW * c_n}{1000},$$

where MW is the molecular weight of glucose (180.16 $gmol^{-1}$).

3.7.2. Biomass concentration

At the end of each flask experiment the remaining volume of the culture was used to perform an OD – cell dry weight analysis. From this volume, 5 different culture solutions were created in a Greiner tube (undiluted, 1:2 diluted, 1:3 diluted, 1:4 diluted, 1:5 diluted). From each solution the OD_{750} was measured in 3 technical replicates. If needed, the sample was diluted with dH_2O. For the further use of the OD_{750} values the average was calculated. Next, two pre-weighed dry glass tubes were each filled with 5ml of a solution. The remaining volume of samples in the Greiner tubes were then centrifuged at 4000 rpm for 3 min. If the supernatant was not turbid and clear of all cells, as determined by microscopy, two pre-weighed dry glass tubes were each filled with 5ml of supernatant. If the culture was not clear filtration was performed to gain a clear and cell free supernatant. The glass tubes were dried at 104 °C over night. The next day the tubes were weighed and the biomass concentration was calculated (see 3.7.3.1. Biomass).

For the fermentations of *Chlorella vulgaris*, the biomass was measured daily with a dry weight analysis. 10 ml of the well mixed culture were transferred into a pre-weighed glass tube as well as 10 ml of the supernatant. The supernatant was gained by centrifugation at 4000 rpm for 5 min. Technical duplicates were performed. The tubes were incubated at 104 °C over night. The next day the tubes were weighed and the biomass was calculated as described in 3.7.3.1. Biomass.

For the fermentations and airlift bioreactor cultivations of *Schizochytrium mangrovei* an OD – biomass correlation graph was continuously used. All the data generated throughout the cultivation experiments (flasks, fermenter, and airlift bioreactor) was used for the correlation

graph. Not only end measurements but also measurements from the beginning of the cultivation as well as the middle were considered to ensure a correct correlation (3.7.3.2. OD - biomass correlation).

3.7.3. Calculation of the key indicators

3.7.3.1. Biomass from dry weight analysis

The biomass concentration c_m in g L^{-1} was calculated by subtracting the mass concentration of supernatant c_S in g L^{-1} and the mass concentration of the culture c_C in g L^{-1}.

$$c_m = c_C - c_S$$

3.7.3.2. OD – biomass correlation

For the OD – biomass correlation the OD_{750} was plotted against the measured biomass concentration. A linear regression was performed, yielding an equation, where the slope *s* and an intercept *i* were used for the calculation of the biomass concentration c_m in g L^{-1}.

$$Absorption = s * c_m + i$$

Rearranging this formula, the biomass concentration can be calculated if the OD_{750} value of a sample is known:

$$c_m = \frac{Absorption}{s} - \frac{i}{s}.$$

3.7.3.3. Biomass productivity

With the biomass concentration the biomass productivity c_{mt} in g $L^{-1}$$day^{-1}$was calculated. Here, the biomass concentration produced over a specific time period Δx was divided by the time Δt in hours needed. To convert this value to biomass produced over 1 day, a multiplication with 24 was included in the calculation.

$$c_{mt} = \frac{\Delta x}{\Delta t} * 24$$

3.7.3.4. Growth rate

From the exponential phase of the growth curve the growth rate μ in day^{-1} was calculated. The natural logarithm of the OD_{750} value at the end exponential phase $OD(t)$ divided by the value at the start exponential phase $OD(0)$ was calculated. This value was divided by the time required for the exponential phase Δt between the end and the beginning of the exponential phase.

$$\mu = \frac{ln\frac{OD(t)}{OD(t0)}}{\Delta t}$$

3.7.3.5. $Yield_{X/S}$

This yield gives the biomass produced per mass unit of substrate consumed. This values can be calculated by using the biomass concentration (x) and the corresponding glucose concentration (s).

$$\frac{\Delta x}{\Delta s} = YieldXS\ [g\ g^{-1}]$$

3.8. Lipid content assay (Sulfo-Phospho-Vanillin assay)

Using this assay, the lipid content of the liquid culture was determined. The principle behind the assay is the reaction of a carboxyl group of the Phospho-Vanillin (PV) solution with a free fatty acid. The hydroxy group of the vanillin reacts with the phosphoric acid resulting in an active aromatic phosphate ester. The sulfuric assay is used to denaturize the cells and the lipid ester bonds (Knight & Anderson, 1972). The described Sulfo-Phospho-Vanillin (SPV) assay was performed after Rische (2015).

For the PV solution, 0.6 g vanillin were dissolved in 10 mL ethanol with a magnetic stirrer on a stirring unit. Next, 90 mL dH_2O and 400 mL phosphoric acid (85%) were added. The solution was stored in a 500 mL glass flask under dark conditions.

To calibrate the assay a standard lipid solution was created. 20 mg of sunflower oil were dissolved in 10 mL Chloroform. From the standard solution different dilutions were created in a glass tube in the range from 0-7 µg mL^{-1}. The Chloroform needs to evaporate completely before continuing. This can be achieved by gassing or slight heating. After the Chloroform evaporated, 100 mL dH_2O were added. The samples were handled identically to the unknown lipid content samples. Once the absorption was known, the OD_{530} was plotted against the lipid concentration. Linear regression yielded an equation with a slope *s* and an intercept *i*:

$$Absorption = s * c_n + i$$

This equation can then be used for the calculation of the glucose concentration c_n in the samples.

For the unknown samples 1 mL of liquid homogenized culture were transferred into a glass tube. 2 mL of sulfuric acid (97%) were added. The tube was closed with a seal and mixed. The glass tube was incubated at 100 °C for 10 min. After the incubation the tube was put on ice for 5 min. After the samples were cooled 5 mL of PV solution were added. The samples were

vortexed. The next step was to incubate at 37 °C for 15 min. After incubation, the samples were cooled by leaving them at room temperature for 30 min in the dark. Before the photometrical measurement the samples were mixed. 1 mL of the sample was transferred into a cuvette. The photometrical measurement was performed at 530 nm. Technical triplets for each sample were done.

For the calculation the average adsorption value was calculated. To get to the mass in µg of lipid, the following calculation was necessary:

$$Lipid\ [\mu g] = \frac{Absorption}{s} - \frac{i}{s}$$

To get to the grams of lipid in1 liter of a culture another calculation was performed:

$$g\ Lipid/L\ culture = Lipid\ [\mu g] * \frac{1}{10^6} * 1000 * \frac{1}{0{,}03}$$

3.9. Lipid extraction

Flask cultures of *Schizochytrium mangrovei* were used for lipid extraction. The culture was homogenized for several rounds at 500 bar. Different organic solvents were used to identify the organic solvent that extracts the most lipid (Table 15).

10 mL of liquid homogenized culture were transferred into a Greiner tube. The documented amount of organic solvent was added to the liquid culture. The mixture was placed inside a water bath which kept the temperature at 60 °C and additionally provided shaking of the tubes to increase the mass transfer between the organic and the aqueous phase. After 2 hours of mixing and heating in the water bath, the Greiner tubes were placed inside a centrifuge for 5 min at 4000 rpm. The organic phase was carefully removed with a glass pipette and transferred into a pre weighed Greiner tube. The tube was placed under the hood overnight to evaporate the organic solvent present in the tube. The next day, the organic solvent had evaporated and the lipid remained inside the Greiner tube and was weighed.

For comparing the weighed values with each other the lipid amount was calculated in g L^{-1}.

Table 15: Organic solvents used for the lipid extraction of *Schizochytrium mangrovei* cultures. The ratio of organic solvent used and culture used is mentioned in the table as well.

Organic solvent	Ratio organic solvent : liquid culture
Hexan	1:1
Methanol	1:1
Petrolether	1:1
Rape seed oil	1:1
$CaCl_2$	1:10
HCl	1:10
H_2SO_4 (+ Methanol : Petrolether)	1:10
Methanol : Hexan	1:2:2
Methanol : Petrolether	1:2:2
Chloroform : Methanol : Water	2:1:2

For a lipid analysis approximately 30 mg of lipid were transferred into a glass tube and sent for analysis to get an insight into the lipid composition of the *Schizochytrium mangrovei* strain cultivated.

4. RESULTS

4.1. Microbiome study

The 18S rRNA amplification was performed to get an insight into the structure of the natural microbiome of environmental microalgae. The samples were taken from places where the presence of microalgae was suspected.

In Figure 12 an overview of all the samples analyzed can be seen on a phylum level. Already at this level, differences of the overall sample groups were evident. The groups 3B and 3C showed a high relative abundance of *SAR* (at least 50 %) which were less represented in the other samples groups. *Archaeplasitida* and *Opis*thokonta represented 50 % of the relative eukaryotic biomass in the other samples investigated. In the sample 3E *Opisthokonta* was the predominant group (90 %).

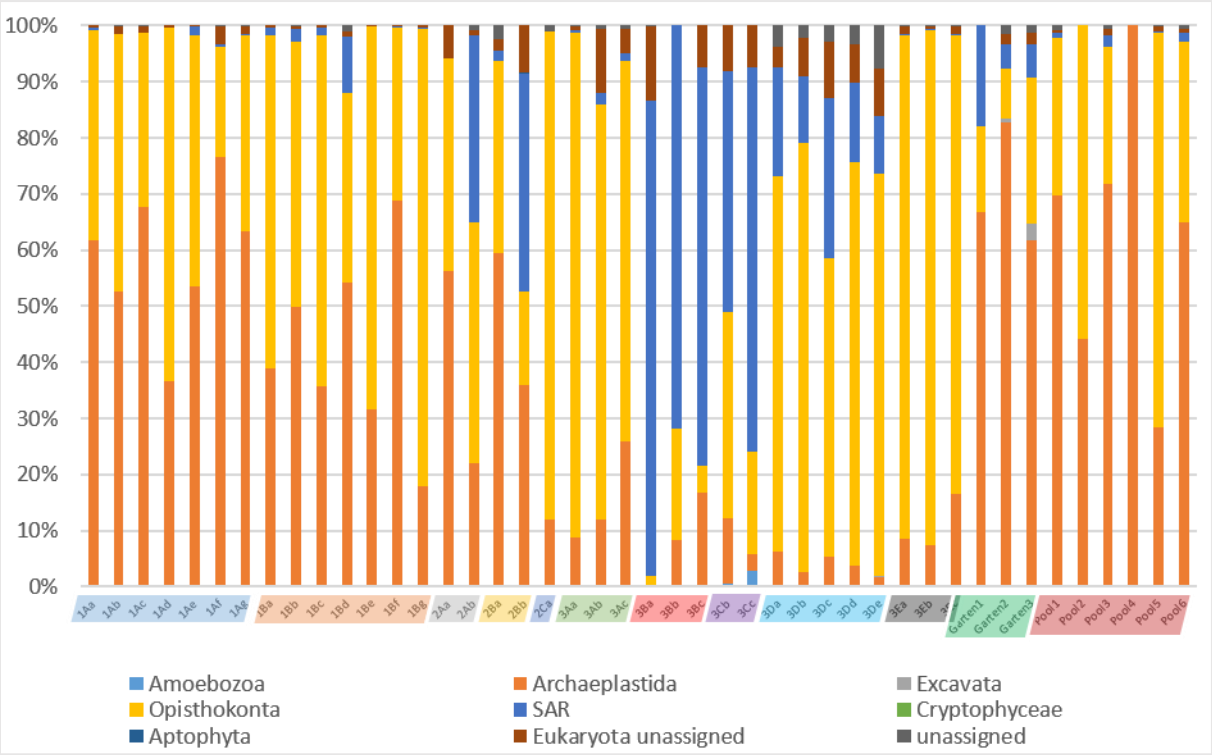

Figure 12: Visualization of all analyzed samples on phylum level . The replicates are grouped by color overlay. light blue: red snowfield, light orange: green snowfield, light grey: pond, light yellow: pond, dark blue: swimming pond, light green: red snowfield, light red: stagnant water, light purple: lake, turquoise: orange snowfield, dark grey: red snowfield, dark green: red biofilm on plastic chair, dark red: tile of a pool

The most frequently found taxon on order level in the samples from Graz and Ennstal was Chloroplastida (~70 %). The order *Holozoa* made up the same amount (~15 %) of Ennstal and Graz. The remaining 15 % differed slightly. Triebener Tauern and Drei Lacken contained ~50 % of *Chloroplastida*. Triebener Tauern showed a higher amount of *Nucletmycea* compared to Drei Lacken. Seetaler Alpen differed from the other locations. The location Graz was the only location to contain *Discoba* (Figure 13).

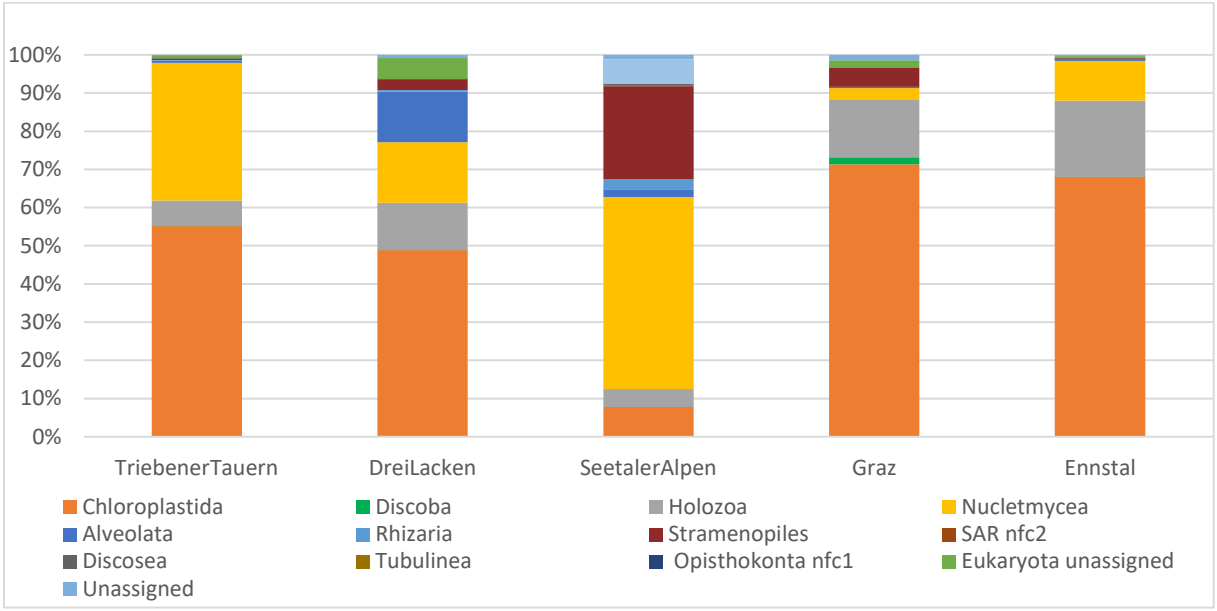

Figure 13: Comparison of microalgae community composition from different locations on order level. The samples of each location were condensed. The locations include Triebener Tauern, Drei Lacken, Seetaler Alpen, Graz and Ennstal. nfc: not further classified

The samples that were taken from snowfields at different locations showed high similarities regarding the main organism groups (Figure 14). Samples snowfield3A, 3D and 3E contained at least 60 % of fungi. Their relative abundance in sample snowfield3D was higher than in the other samples. Sample snowfield1A and 1B had approximately 50 % of *Chlorophyta* and about 30 % of fungi. The overall dominating taxonomic group on the snowfields belonged to fungi.

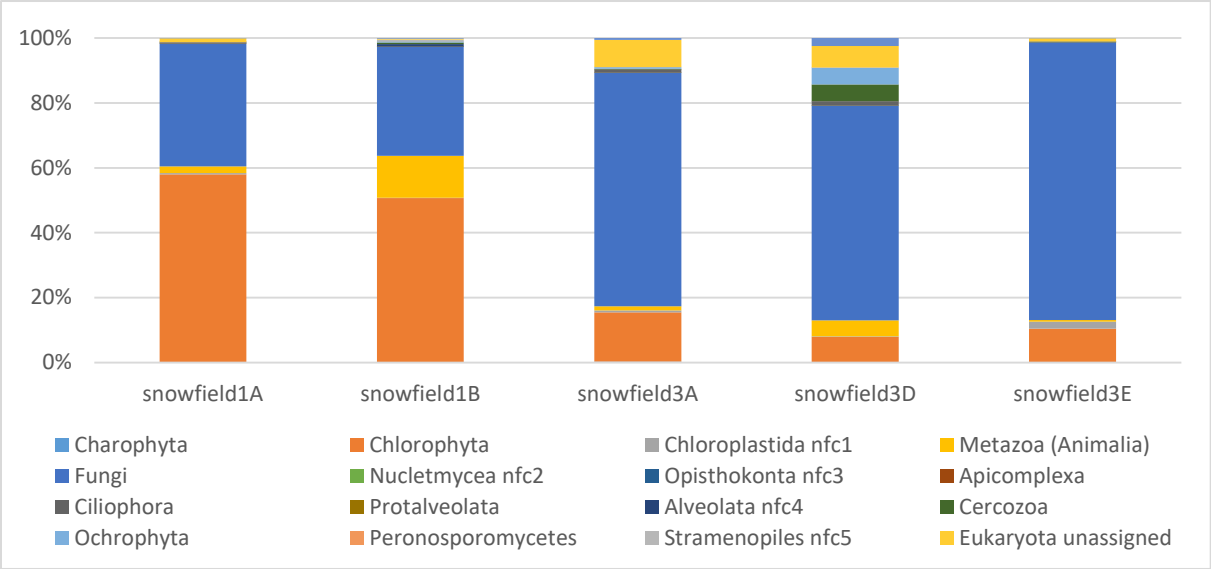

Figure 14: Comparison of snowfield samples on the order level . The replicates of each snowfield were condensed. The samples include two snowfield samples from Triebener Tauern (snowfield1A, snowfield1B) and three snowfield samples from Seetaler Alpen (snowfield3A, snowfield3D, snowfield3E). nfc: not further classified

The microbiome of the water samples on order level are displayed in Figure 15. Within the samples lake2A and 2B over 40 % of *Chlorophyta* were detected. The other samples also showed the presence of *Chlorophyta* but to a lesser extent. Sample 2C contained 60 % of fungal ribosomal sequence variants (RSVs) whilst sample water3B contained over 60 % of *Ochrophyta*. Sample lake3C showed the highest abundance. The biggest group in sample lake3C was *Chloroplastida* nfc3 (70 %). This group wasn´t that well represented in the other samples. Similar to the snowfield samples, the group of fungi is also well represented in all the water samples.

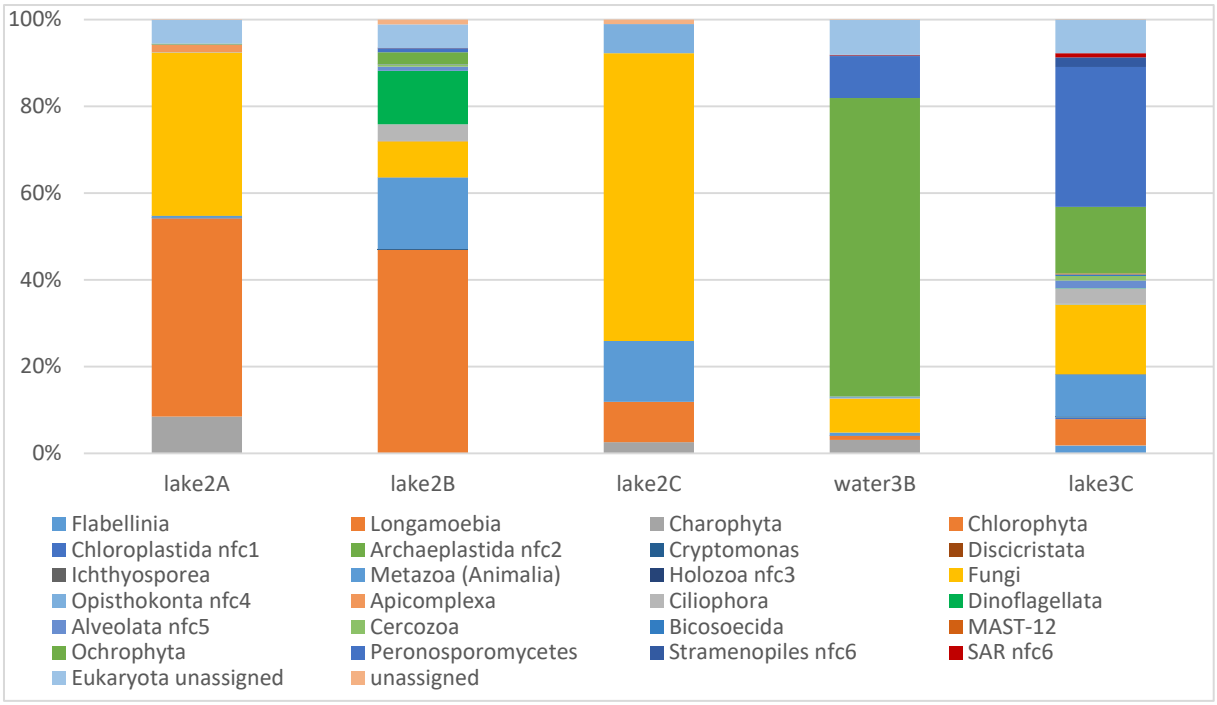

Figure 15: Comparison of water samples on order level . The replicates of each water samples were condensed. The samples include tree samples from Drei Lacken (lake2A, lake2B, lake2C) and two samples from Seetaler Alpen (water3B, lake3C) nfc: not further classified

The two samples spots which were not natural habitats for microalgae were the plastic chair and the tile of a pool (Figure 16). In both cases *Charophyta* represented at least 60 %. *Discicristata* were present with at least 15 % in the urban habitats. The eukaryotes that did only show up in the urban habitats were *Dictyostelium* and *Arcellinida*.

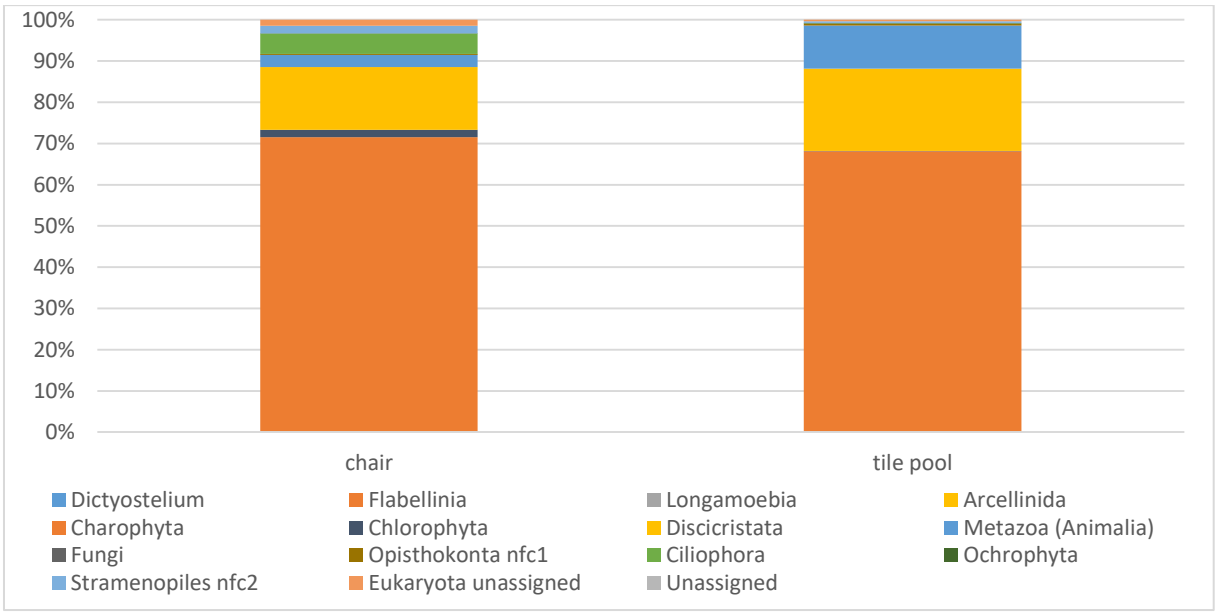

Figure 16: Comparison of the unnatural habitat samples on the order level. The non-environmental habitats include a white plastic chair and the tile of a pool. The replicates of each samples were condensed. The chair sample was taken in Graz, the tile pool sample was taken in Ennstal. nfc: not further classified

The alpha – rarefaction plot revealed a high diversity of the samples 2B and 3C (Figure 17). The lowest diversity was represented with the samples 1B, 3B and pool. The samples 1A and chair were not as diverse as samples 3D and 3A.

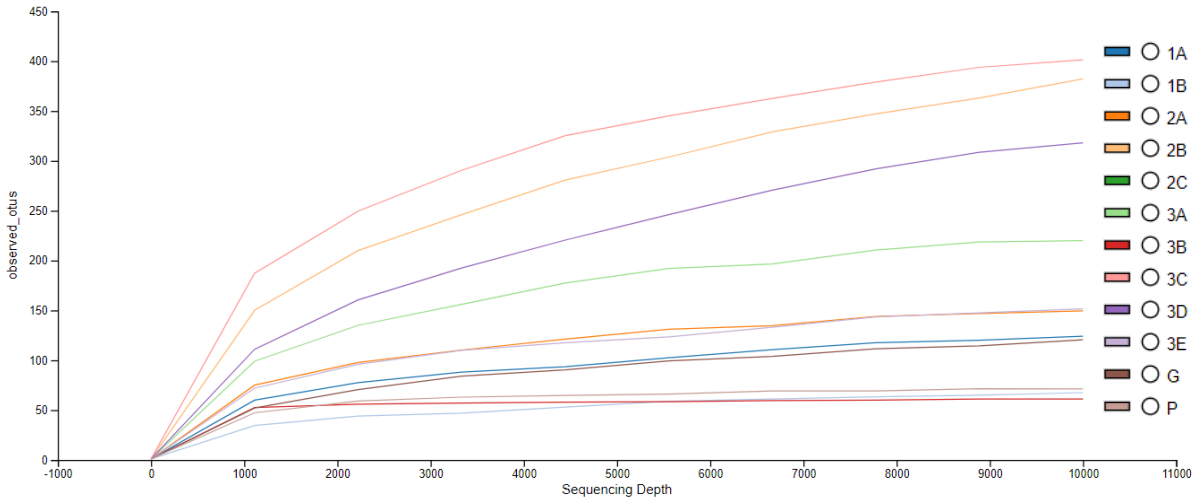

Figure 17: Alpha-rarefaction graph of the sequenced samples. Observed OTUs are an indicator for the microbial diversity in the samples.

The PCOA plot showed the similarities of the samples with each other and can be seen in Figure 18. All snowfield samples were grouped with other snowfield samples. 2 replicates of samples snowfield1A were located near snowfield1B. The replicates of sample lake2A were very close to the rest of the snowfield1A samples. The chair samples were grouped nicely as well as the lake2B, water3B and lake3C samples. Samples snowfield3E and snowfield3A were very near to each other. The pool samples were located near the chair samples.

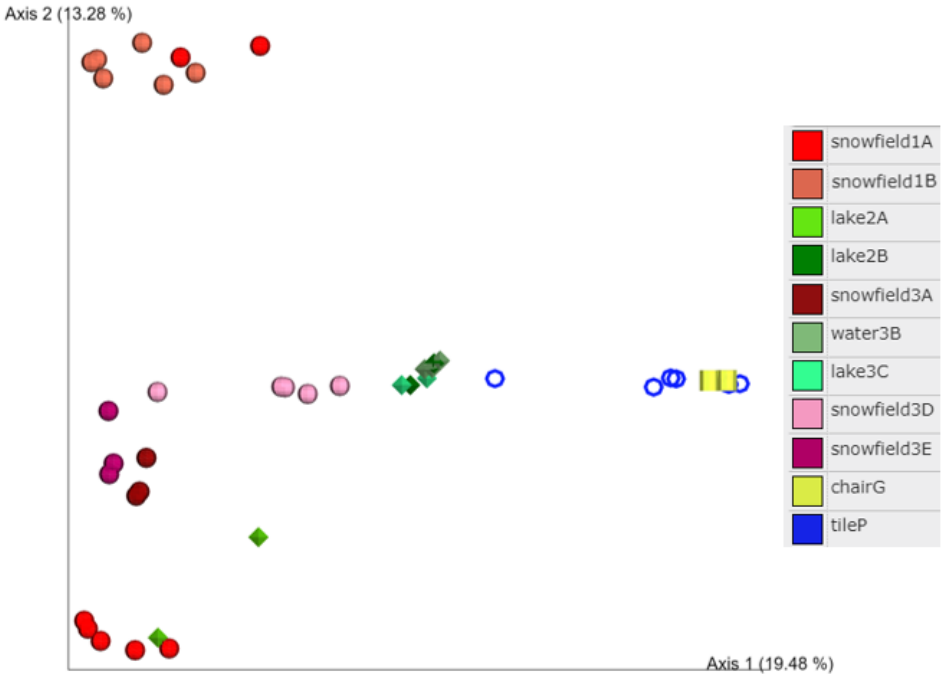

Figure 18: PCOA plot of different amplicon sequencing samples. Samples from the same sampling site are highlighted in the same color for better differentiation.

4.2. Growth and biomass determinations under heterotrophic cultivation

4.2.1. Substrate concentration

The cultivation with different glucose concentrations was documented. From the collected data individual growth curves were created. In addition to the biomass concentration the glucose concentration was plotted on the graphs.

4.2.1.1. Chlorella vulgaris

Chlorella vulgaris was cultivated on different substrate concentrations to identify the ideal glucose concentration for the microalgae´s growth.

A substrate concentration of 40 g L^{-1} glucose did not inhibit the microalgae´s growth. This growth curve can be seen in Figure 19A. a very short lag phase of a couple of hours was documented, followed by an exponential phase which lasted until hour 70. After 70 hours the cell growth stagnated. At hour 160 a slight increase in the biomass concentration was noted. After this, the biomass concentration declined. The glucose provided was consumed entirely.

The cultivation with a substrate concentration of 60 g L^{-1} glucose did behave similarly. In comparison to the growth curve in Figure 19A, a longer lag phase of 20 hours was observed. Followed by an exponential phase which lasted until hour 70. After 70 hours the biomass concentration declined. The glucose curve revealed the complete consumption of the provided substrate which can be seen in Figure 19B.

The growth curve of the different substrate concentrations did show that at a higher substrate concentration (80 g L^{-1} glucose) inhibition was present (**Figure 19**C). The growth of the microalgae didn´t start as fast in comparison to lower glucose concentrations. The microalgae grew slowly. After 150 hours the growth stagnated, even though there was still glucose present. After 180 hours the cultivation was stopped. The cultivation was stopped with 15 g L^{-1} glucose still remaining in the medium.

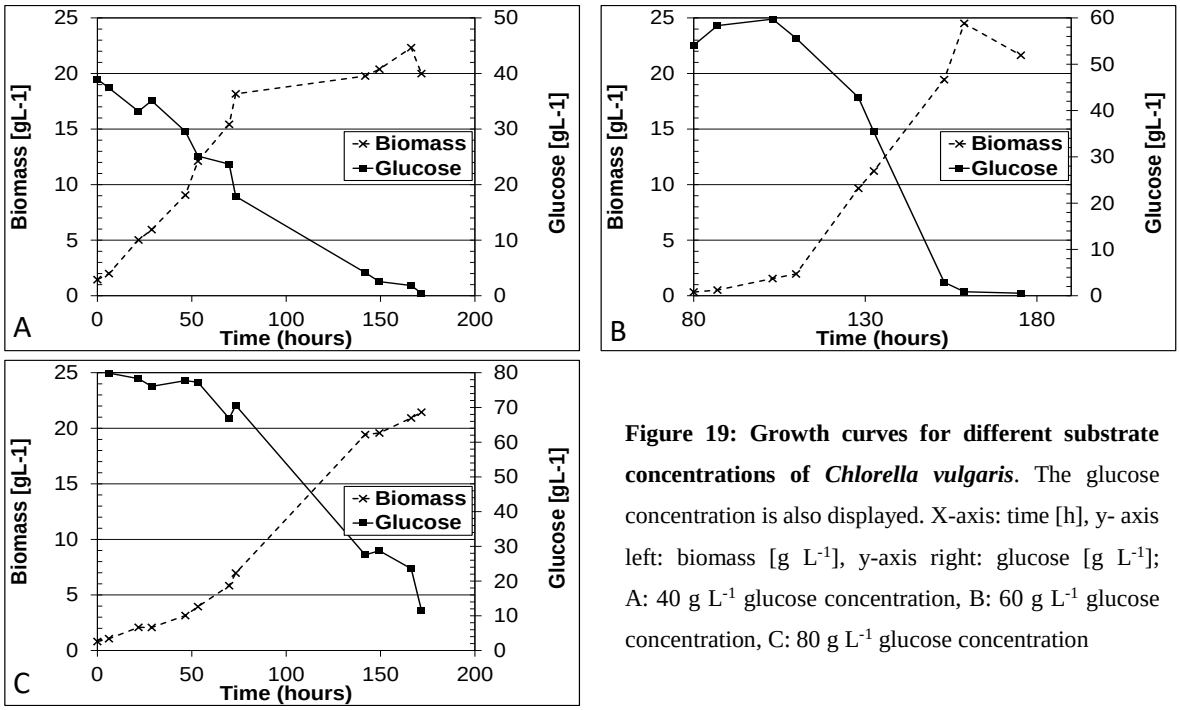

Figure 19: Growth curves for different substrate concentrations of *Chlorella vulgaris*. The glucose concentration is also displayed. X-axis: time [h], y- axis left: biomass [g L^{-1}], y-axis right: glucose [g L^{-1}]; A: 40 g L^{-1} glucose concentration, B: 60 g L^{-1} glucose concentration, C: 80 g L^{-1} glucose concentration

Data obtained from the substrate experiments supported the information gained from the growth curves. At a glucose concentration of 80 g L^{-1}, the biomass, biomass productivity, yield and growth rate were lower than for 40 g L^{-1} and 60 g L^{-1}. The cultivation with 60 g L^{-1} glucose did generate the highest numbers for each key indicator expect for the yield. Here, the 40 g L^{-1} glucose cultivation did reach the best value with 0.793 g of cell mass per gram of glucose. The calculated key indicators are presented in Table 16.

Table 16: Calculated key indicators for the substrate concentration experiments of *Chlorella vulgaris* . The key indicators include the max. biomass concentration, the growth rate, the biomass productivity and the yield.

Glucose	**Biomass (max.)**	**μ (exponential phase)**	**Biomass productivity**	**$Y_{X/S}$**
[g L^{-1}]	[g L^{-1}]	[day^{-1}]	[g L^{-1} day^{-1}]	[g g^{-1}]
40	22.320	0.791	5.474	0.793
60	24.507	0.880	7.201	0.454
80	21.44	0.537	2.855	0.290

4.2.1.2. Growth experiments with *Schizochytrium mangrovei*

4.2.1.2.1. Nitrogen source

To improve the growth of *Schizochytrium mangrovei* different nitrogen sources were tested.

The cultivation with 30 mM $(NH_4)_2SO_4$ showed an increase in the biomass within 50 hours. After that, the growth reached a plateau for 15 hours and then the biomass concentration declined. Overall, the growth seemed to be progressing at the beginning of the cultivation but stopped after hour 60 (

The microalgal growth on 30 mM Urea showed a short lag phase of 8 hours. After this, the exponential phase started and lasted until hour 50 (Figure 20B). Then, the biomass concentration declined. The glucose curve showed the consumption of the entire substrate provided. The key indicators associated with this cultivation experiment yielded higher values than the cultivation with $(NH_4)_2SO_4$ which can be seen in Table 17. A biomass concentration of 32.9 g L^{-1} was produced. The pH measurements during the cultivation revealed a slight decrease of the pH value during the cultivation. The lowest pH measured was 5.5 which seemed to be tolerable for the microalgae. Microscopy did not show any cell debris but intact cells, where the life cycle of the microalgae was observable.

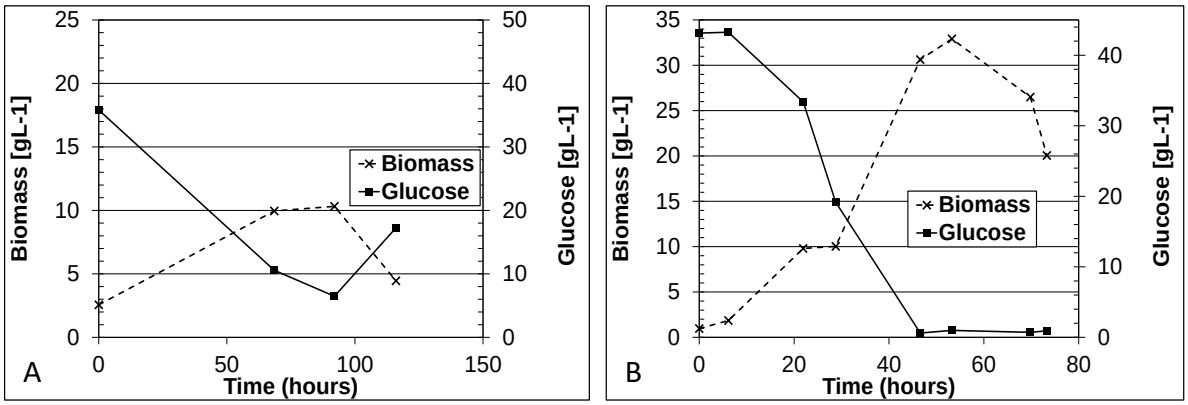

Figure *20*A). The microalgal cells were not able to consume the entire substrate provided. Only half of the glucose was consumed by the cells. The corresponding key indicators as seen in **Table *17*** revealed low values for each key indicator. The microscopy showed a destroyed cell culture after hour 60 (Figure 21). No intact cells were observable. Cell debris was floating in the cultivation medium. The pH measurement documented a drastic pH drop during the cultivation. The initial pH value of 7 slightly decreased in the first 50 hours. After hour 50 the pH value dropped down to 2.

The microalgal growth on 30 mM Urea showed a short lag phase of 8 hours. After this, the exponential phase started and lasted until hour 50 (Figure 20B). Then, the biomass concentration declined. The glucose curve showed the consumption of the entire substrate provided. The key indicators associated with this cultivation experiment yielded higher values than the cultivation with $(NH_4)_2SO_4$ which can be seen in Table 17. A biomass concentration of 32.9 g L^{-1} was produced. The pH measurements during the cultivation revealed a slight decrease of the pH value during the cultivation. The lowest pH measured was 5.5 which seemed to be tolerable for the microalgae. Microscopy did not show any cell debris but intact cells, where the life cycle of the microalgae was observable.

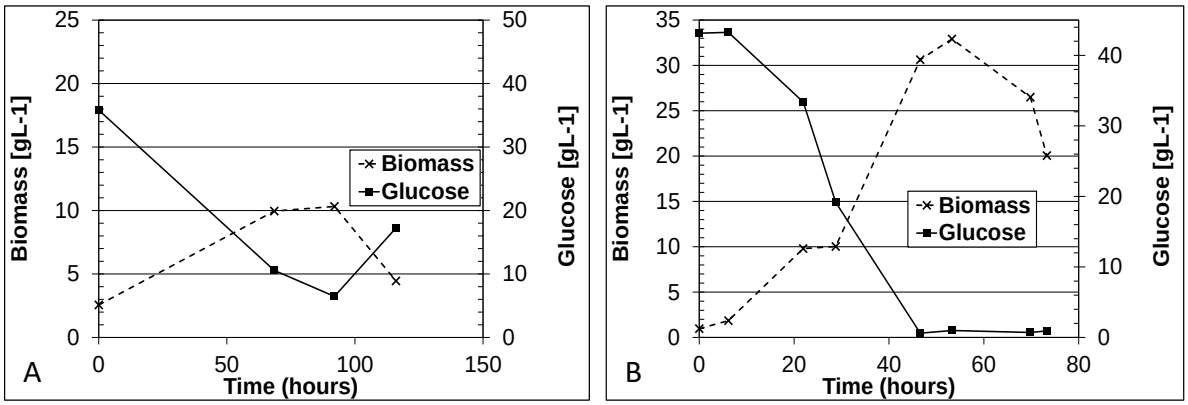

Figure 20: Growth curve and glucose concentration curve of *Schizochytrium mangrovei* using (A) $(NH_4)_2SO_4$ and (B) Urea as a nitrogen source . X-axis: time [hours], y- axis left: biomass [g L^{-1}], y-axis right: glucose [g L^{-1}]

Table 17: Calculated key indicators for the different nitrogen sources of *Schizochytrium mangrovei* . The key indicators include the max. biomass concentration, the growth rate, the biomass productivity and the yield.

Nitrogen source	**Biomass (max.)**	**μ (exponential phase)**	**Biomass productivity**	**$Y_{X/S}$**
	[g L^{-1}]	[day^{-1}]	[g L^{-1} day^{-1}]	[g g^{-1}]
$(NH_4)_2SO_4$	10.322	0.363	2.023	0.264
Urea	32.913	1.664	14.385	0.452

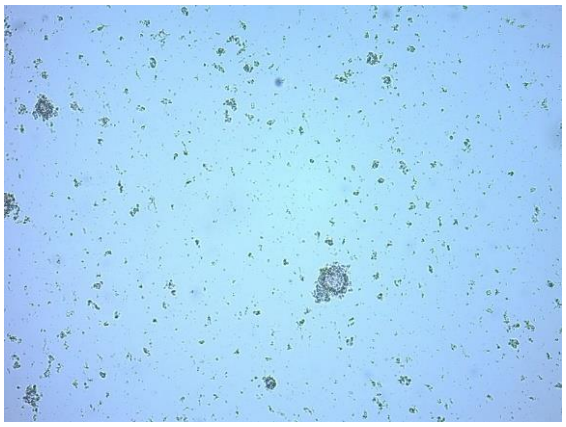

Figure 21: *Schizochytrium mangrovei* after 60 hours of cultivations with $(NH_4)_2SO_4$ as a nitrogen source. The microscopy showed a destroyed cell culture. No intact cells were visible. Cell debris was detected during microscopic evaluation. It showed the microalgae with 600x magnification

Schizochytrium mangrovei was not able to grow with $(NH_4)_2SO_4$ due to the drastic pH drop during the cultivation. For further cultivation of the microalgae, 30 mM Urea was used which led to high key indicator values.

4.2.1.2.2. Substrate concentration

Schizochytrium mangrovei was cultivated on different substrate concentrations to identify the ideal glucose concentration for the microalgae´s growth.

For the cultivation of *Schizochytrium mangrovei* using 40 g L^{-1} glucose a nice growth curve could be created (Figure 22A). A very short lag phase was noticed. The biomass concentration increased within the first 40 hours with a nice exponential phase which lasted up until hour 50. At hour 50, the glucose was completely used up and the biomass concentration declined.

The cultivation with 60 g L^{-1} glucose showed a different behavior of the microalgae (Figure 22 B). The biomass increased in the beginning a little slower than for the lower glucose concentration. After the short lag phase the growth reached the start of the exponential growth phase. After 70 hours the biomass concentration plateaued, even though there was still 10 g L^{-1} glucose present. The microalgae was not able to consume the entire glucose.

The cultivation with 80 g L^{-1} glucose revealed a short lag phase followed by an exponential growth phase. At hour 50 the exponential phase ended and the growth curve reached a plateau. The microalgal culture did not grow further. (Figure 22C). The glucose was not used up entirely, after 50 hours 30 g L^{-1} glucose were still present in the medium.

The cultivation experiment with 120 g L^{-1} glucose showed a longer lag phase compared to the other substrate experiments conducted. The cultivation took over 300 hours. During this time

the cells were able to use up 75% of the initial glucose concentration but the growth was very slow (Figure 22D). A longer time period did allow the cells the take up of the glucose but the time needed for the consumption was very long.

Table 18*:* Calculated key indicators for the substrate concentration experiments of *Schizochytrium mangrovei* . The key indicators include the max. biomass concentration, the growth rate, the biomass productivity and the yield.

Glucose	**Biomass (max.)**	**μ (exponential phase)**	**Biomass productivity**	**$Y_{X/S}$**
[g L^{-1}]	[g L^{-1}]	[day^{-1}]	[g L^{-1} day^{-1}]	[g g^{-1}]
40	32.913	1.664	14.385	0.452
60	37.829	1.241	10.158	0.728
80	33.832	1.014	11.286	0.705
120	34.334	0.172	2.782	0.236

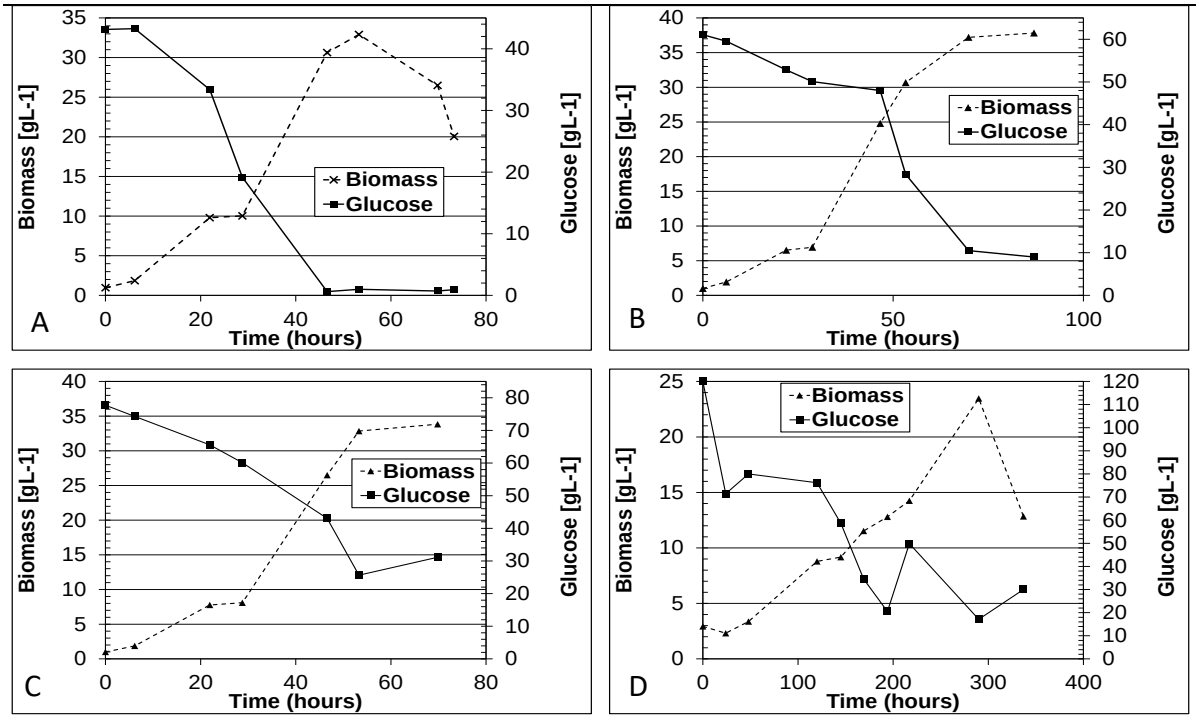

Figure 22: Growth curves for different substrate concentrations of *Schizochytrium mangrovei*. The glucose concentration is also displayed. X-axis: time [h], y- axis left: biomass [g L^{-1}], y-axis right: glucose [g L^{-1}]; A: 40 g L^{-1} glucose concentration, B: 60 g L^{-1} glucose concentration, C: 80 g L^{-1} glucose concentration, D: 120 g L^{-1} glucose concentration

The data gained from the cultivation experiments showed a significant difference between the glucose concentrations used (Table 18). The cultivation with 60 g L^{-1} led to the highest biomass concentration with 37.8 g L^{-1} but the culture was not able to use up the entire substrate within 90 hours, making the other key indicator values lower except the yield. The yield gained from

60 g L^{-1} glucose showed the highest value for all substrate concentration experiments with 0.728 g g^{-1}. The 40 g L^{-1} glucose cultivation consumed the substrate completely. However, the lowest biomass concentration of 32.9 g L^{-1} was produced. The highest values for growth rate and biomass productivity were created for the cultivation with 40 g L^{-1} glucose. The cultivation with 120 g L^{-1} glucose led to a biomass concentration of 34.3 g L^{-1}. However, the time needed to produce this amount relativized the results.

4.3. Batch fermentation experiments

4.3.1. Chlorella vulgaris

The fermentation of *Chlorella vulgaris* differed from the cultivation in the shaking flasks. Three batch fermentations were performed.

The growth curve for the first fermentation is displayed in Figure 23. The fermentation lasted about 50 h, which was twice as fast as the shaking flask cultivation. With the little data points available, no lag phase could be observed, but the biomass concentration increased exponentially starting from the beginning. The biomass growth did not stagnate. However, the provided glucose was completely consumed.

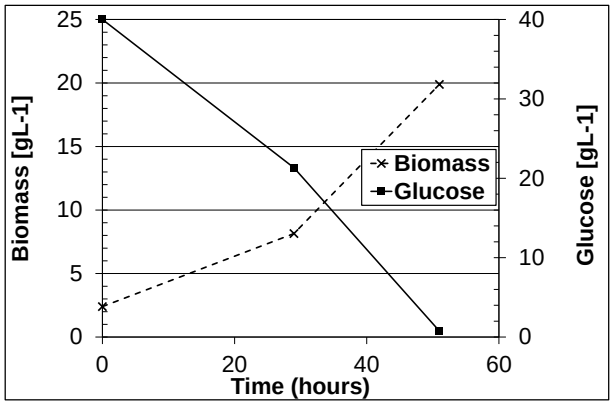

Figure 23: Growth and glucose concentration curve of batch fermentation 1 of *Chlorella vulgaris* . The glucose concentration is also displayed. X-axis: time [h], y- axis left: biomass [g L^{-1}], y-axis right: glucose [g L^{-1}]

The data gained from the first fermentation attempt revealed a lower biomass concentration and yield compared to the shaking flask cultivations. A biomass concentration of 19.9 g L^{-1} was reached (Table 19). Due to the short time needed for the entire consumption of the substrate, the growth rate and the biomass productivity value were higher than for the flask cultivations.

The online data received during the first fermentation process (Figure 24) showed the regulatory steps taken by the controlling unit of the fermenter. After 1 hour the first regulation step of the pO_2 regulation cascade occurred. The airflow (red line in Figure 24) from 2 to 10 NL min^{-1} increased within 4 hours. Next, the stirrer speed and pressure increased to keep the pO_2 at the desired value.

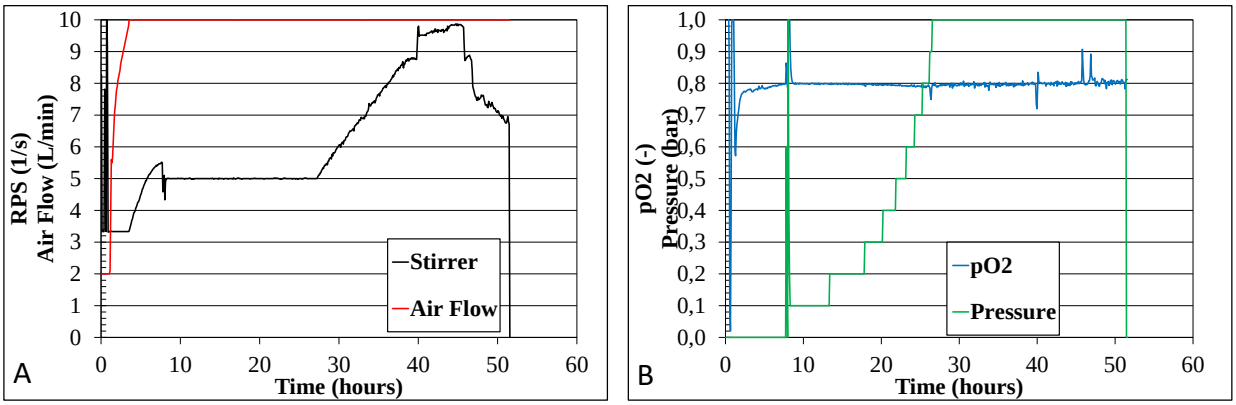

Figure 24: Documented fermentation data from *Chlorella vulgaris* fermentation 1 . Including the (A) stirrer speed, air flow, (B) pO_2 value and pressure change during the fermentation.

The microscopy of the cells during the fermentation Figure 25A showed cell debris, which might explain the lower biomass concentration. Other than that, the culture appeared to be axenic. In Figure 25B, the culture on the final day can be seen. The culture consisted of a variety of cell sizes, no cell division was documented.

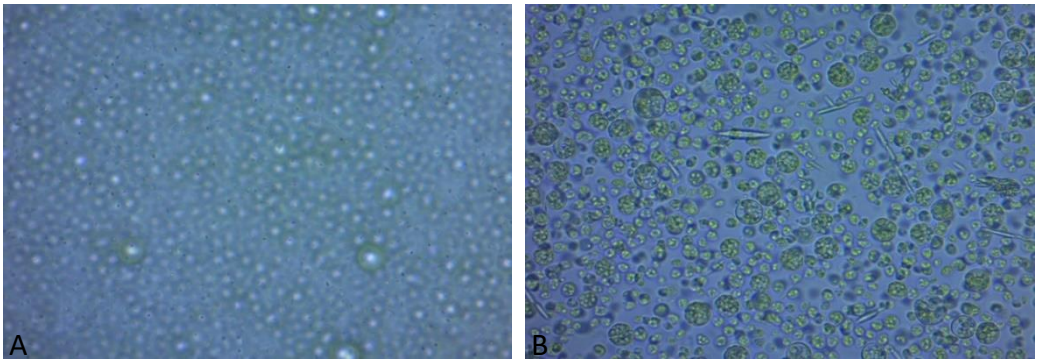

Figure 25: Microscopy picture of *Chlorella vulgaris* during fermentation 1 . (A) showed the cell debris in the background of the cell culture. (B) Showed the general state of the culture after 50 hours. It showed the microalgae with 600x magnification

For the second fermentation the pO_2 cascade was adjusted (flow [2-10 NL min^{-1}] – pressure [0-1 bar] – stirrer [100-500 rpm]). This time the growth curve revealed a lag phase of 18 h. After this, the culture exhibited exponential growth behavior. At hour 40 the cultivation was stopped (Figure 26), due to the declining pO_2 value (Figure 27B). The culture did not use up the entire glucose provide, 8 g L^{-1} glucose were still present in the medium. The key indicators calculated from the second fermentation showed similar values as for the first fermentation Table 19.

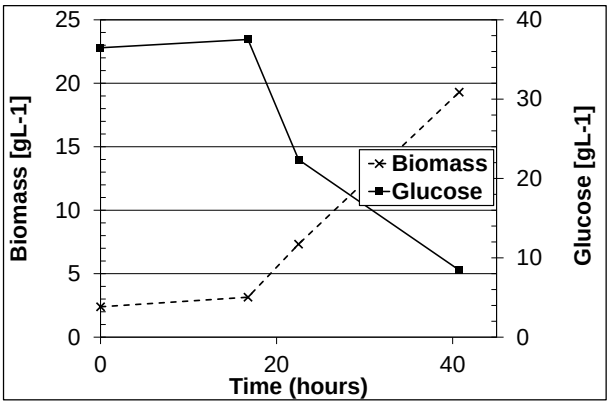

Figure 26*:* Growth and glucose concentration curve of batch fermentation 2 of *Chlorella vulgaris* . The glucose concentration was also displayed. X-axis: time [h], y- axis left: biomass [g L^{-1}], y-axis right: glucose [g L^{-1}]

The recorded data of the fermentation showed the regulatory steps taken from the fermenter system (Figure 27). After ~10 hours the first regulation step, the air flow, reached its maximum. That was when the next regulator step, pressure regulation, occurred. Within 10 hours the pressure increased to 1 bar. This resulted in the third regulatory step, the increase of the stirrer speed. Once the highest allowed stirrer speed of 500 rpm was reached, the pO_2 value decreased which limited the oxygen supply to the microalgal cell culture.

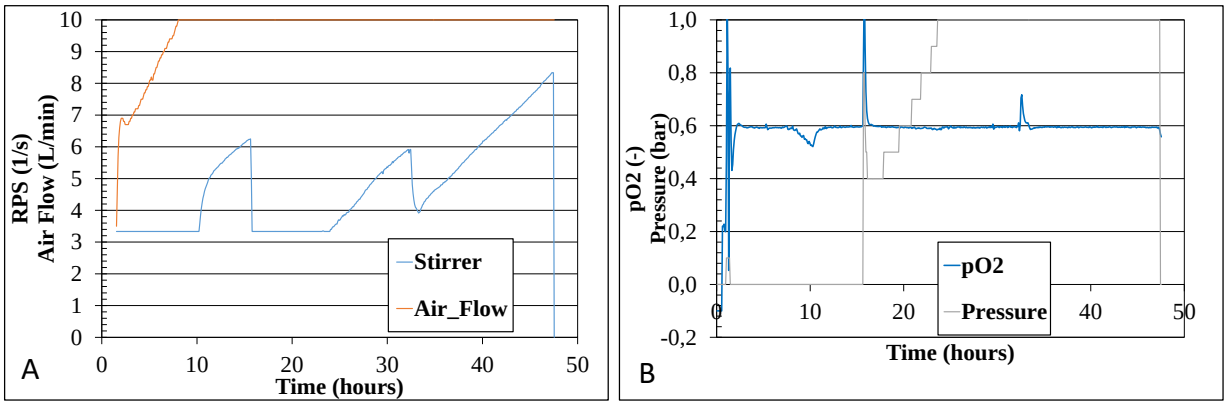

Figure 27: Documented fermentation data from *Chlorella vulgaris* fermentation 2 . Including the (A) stirrer speed, air flow, (B) pO_2 value and pressure change during the fermentation.

The third fermentation attempt was not suitable for analysis due to a leakage in the acid pump tube. The system was open and the pH value was not adjusted for several hours. Due to the possible contamination and the uncontrolled conditions, the fermentation was stopped. The whole fermentation process lasted 15 hours. The key indicators for the third fermentation can be seen in Table 19. All values calculated were lower than for to the other *Chlorella vulgaris* fermentations because the fermentation was not finished. Therefore, this values were not considered for further evaluation.

Table 19*:* Calculated key indicators for the batch fermentations of *Chlorella vulgaris* . The key indicators included the max. biomass concentration, the growth rate, the biomass productivity and the yield.

	Biomass (max.)	**μ (exponential phase)**	**Biomass productivity**	**$Y_{X/S}$**
	[g L^{-1}]	[day^{-1}]	[g L^{-1} day^{-1}]	[g g^{-1}]
Fermentation 1	19.890	1.438	8.235	0.446
Fermentation 2	19.295	2.159	9.953	0.861
Fermentation 3	7.595	1.975	2.594	1.324

Overall, the highest biomass concentration was produced with the first fermentation. The highest growth rate, biomass productivity and yield were achieved in the second fermentation.

4.3.2. Schizochytrium mangrovei

The three batch fermentations conducted with *Schizochytrium mangrovei* did not reflect the observed characteristics of the microalgae and key indicators observed in the flask experiments.

The three fermentations showed the same growth inhibition of the microalgae as well as similar key indicators. Each fermentation was performed over 130 hours. The growth curves for each fermentation were similar (Figure 28). The microalgae grew very slowly starting from the beginning. The growth did not reach an exponential phase. The growth curves revealed a very slow substrate uptake as well. After 130 h only 10 g L^{-1} glucose were consumed by the microalgae. The highest biomass concentration gained from all fermentations was 7.8 g L^{-1} (Table 20). That was significantly lower than the values from the shaking flask experiments. Additionally, also the growth rates, biomass productivities and yields were lower. The growth of *Schizochytrium mangrovei* seemed to be inhibited in each fermentation attempt.

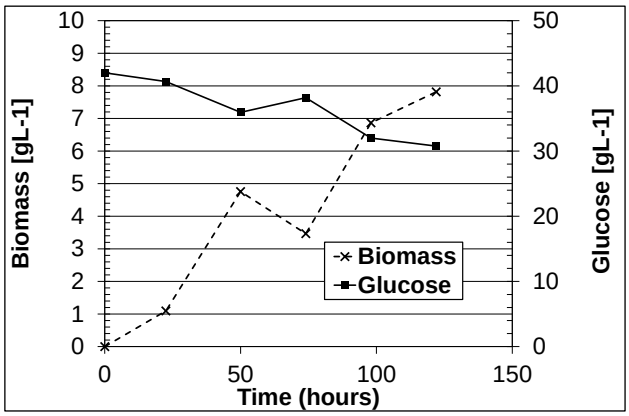

Figure 28*:* Growth and glucose concentration curve of batch fermentation 6 of *Schizochytrium mangrovei* . The glucose concentration was also displayed. X-axis: time [h], y- axis left: biomass [g L^{-1}], y-axis right: glucose [g L^{-1}]

Table 20: Calculated key indicators for the batch fermentations of *Schizochytrium mangrovei* . The key indicators include the max. biomass concentration, the growth rate, the biomass productivity and the yield.

	Biomass (max.)	**μ (exponential phase)**	**Biomass productivity**	**$Y_{X/S}$**
	[g L^{-1}]	[day^{-1}]	[g L^{-1} day^{-1}]	[g g^{-1}]
Fermentation 5	2.966	0.782	0.578	0.362
Fermentation 6	7.815	0.471	1.537	0.610
Fermentation 7	3.945	0.466	0.546	0.153

The fermentation documentation graphs of all three fermentations showed similar results. The fermentation documentation graph of fermentation 6 was displayed in **Figure *29***. They revealed no increase in oxygen demand, which was the result of a low biomass concentration in the fermenter. No regulatory steps to maintain the pO_2 saturation were activated. The sterility of the culture was confirmed by microscopy (**Figure *30***). No mobile cells were detected, which was a result of no growth. In comparison to the shaking flask experiments, the culture was not dense. During the fermentation process something inhibited the microalgae´s growth. To identify the inhibiting factor, experiments in an airlift bioreactor were conducted.

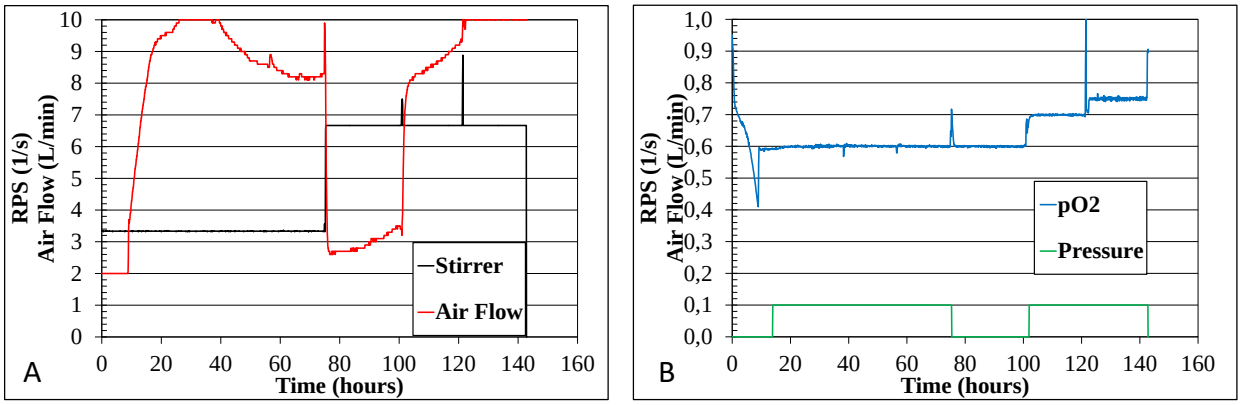

Figure 29: Documented fermentation data from *Schizochytrium mangrovei* fermentation 6 . Including the (A) stirrer speed, air flow, (B) pO2 value and pressure change during the fermentation.

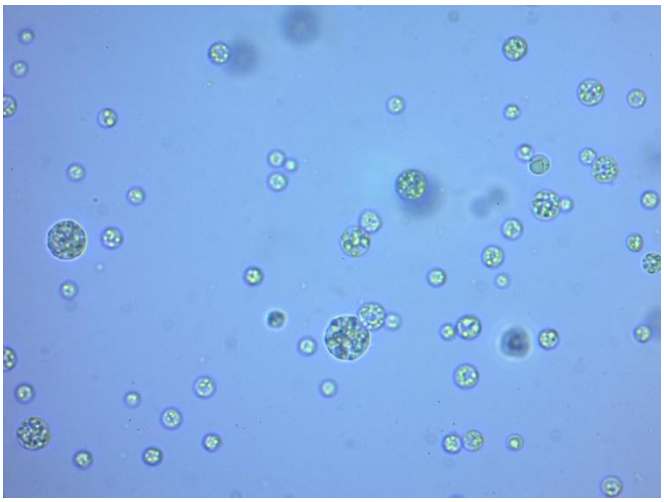

Figure 30*:* Microscopy picture of *Schizochytrium mangrovei* during fermentation 6 . The microscopy picture showed more smaller cells than larger ones. However, no mobile cells were observed. It showed the microalgae with 600x magnification

4.4. Airlift bioreactor experiments

Cultivation experiments in the airlift bioreactor were conducted to investigate the inhibited growth of *Schizochytrium mangrovei* in the fermentation processes. Two different experiments were performed: One to simulate the fermentation cultivation and try to reproduce the problem, and the second one to eliminate the inhibitor.

4.4.1. Fermentation simulation

The first approach, where the airlift bioreactor was treated like the fermenter (medium components except for glucose were autoclaved twice inside the bioreactor) the bioreactor showed the same behavior as the fermenter (Table 21), i.e. the growth of the microalgae was inhibited. The culture did not reach an exponential phase. The slow growth stagnated after 100 hours, no significant increase in the biomass concentration was documented after that. The cultivation was stopped after 200 hours. The glucose curve in Figure 31 did decline slowly. The culture did consume 15 g L^{-1} of the provided glucose. A biomass of 7.2 g L^{-1} after 200 h was produced, which is a little less biomass than in the fermenter.

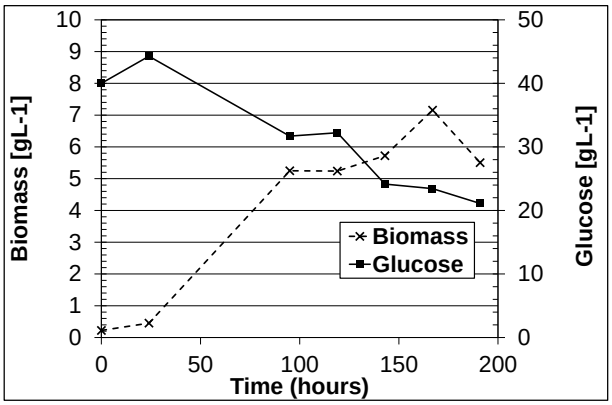

Figure 31*:* **Growth and glucose concentration curve of the fermentation simulation in an airlift bioreactor of *Schizochytrium mangrovei*** . The glucose concentration was also displayed. X-axis: time [h], y- axis left: biomass [g L^{-1}], y-axis right: glucose [g L^{-1}]

Table 21*:* Calculated key indicators for the fermentation simulation in an airlift bioreactor of *Schizochytrium mangrovei* . The key indicators included the max. biomass concentration, the growth rate, the biomass productivity and the yield.

Biomass (max.)	**μ (exponential phase)**	**Biomass productivity**	**$Y_{X/S}$**
[g L^{-1}]	[day^{-1}]	[g L^{-1} day^{-1}]	[g g^{-1}]
7.157	0.499	0.997	0.419

When the medium handling of the flask experiments and the fermentations were compared, a difference was noticed. The shaking flasks were filled with sterile filtered medium, whereas the fermenter and fermenter simulation experiment were filled with heat sterilized medium (30 min, 121 °C). This difference led to the assumption of a nutrition limitation in the fermenter and the fermenter simulation experiment, which could explain the lower key indicators.

To confirm this theory, the same cultivation in an airlift was performed with a sterile filtered medium.

4.4.2. Sterile filtration experiment

In the growth curve obtained from the cultivation with the sterile filtered medium, the culture reached the exponential phase (Figure 32). In the beginning of the cultivation, the growth of the microalgae was slow, however, within the first 50 hours a biomass concentration of 6 g L^{-1} was produced, which was more biomass when compared to the 4.4.1. Fermentation simulation experiment. At hour 80 the oxygen supply was increased manually from 0.5 L min^{-1} to 1 L min^{-1}. After this oxygen boost, the culture was able to use up the glucose and produce a biomass of 23.8 g L^{-1} within 120 h.

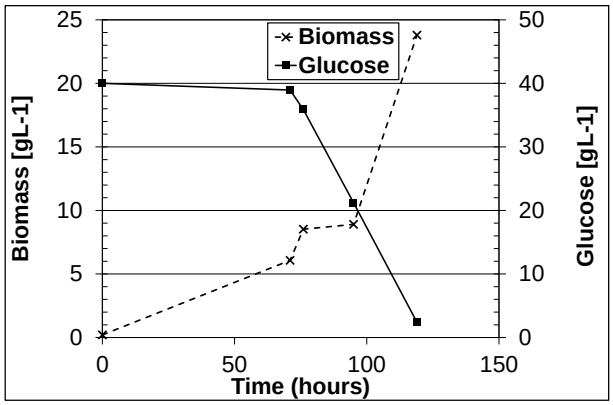

Figure 32: Growth and glucose concentration curve of the sterile filtered medium experiment in an airlift bioreactor of *Schizochytrium mangrovei* . The glucose concentration was also displayed. X-axis: time [h], y- axis left: biomass [g L^{-1}], y-axis right: glucose [g L^{-1}]

Table 22: Calculated key indicators of the sterile filtered medium experiment in an airlift bioreactor of *Schizochytrium mangrovei* . The key indicators included the max. biomass concentration, the growth rate, the biomass productivity and the yield.

Biomass (max.)	**µ (exponential phase)**	**Biomass productivity**	**$Y_{X/S}$**
[g L^{-1}]	[day^{-1}]	[g L^{-1} day^{-1}]	[g g^{-1}]
23.792	0.573	4.799	0.633

The key indicators obtained for this cultivation can be seen in Table 22. With the sterile filtered medium, a higher biomass concentration, growth rate, biomass productivity and yield were reached than for all fermentation experiments. In comparison to the flasks experiments, the key indicators were lower, which can be explained by the uncontrolled conditions within the bioreactor. The pH value was not stable over time. Due to the manual correction the pH sank down to a value of 4 before being corrected to 7. Additionally, the oxygen supply was not increased exponentially with the growth.

The cultivation with the airlift bioreactor and sterile filtered medium confirmed the suspected nutrition limitation from the fermenter simulation experiment and also revealed an oxygen limitation inside the airlift bioreactor system.

4.5. Lipid content assay

4.5.1. Lipid content

The lipid content of the 5 L cultivations of *Schizochytrium mangrovei* was determined with an SPV assay. The lipid content in g L^{-1} and the percentage of the lipid of the culture can be seen in Table 23. The assay did show a very high lipid content for the cultures. The minimum lipid content calculated was 40 % whereas the highest was 60 %. The high lipid content seemed to be independent of the culture density. Cultures with a lower biomass concentration, like fermentation 6, as well as culture with a higher biomass concentration - like airlift 3 - had a high lipid content.

Table 23: Results of the SPV assay of the 5L cultivations of *Schizochytrium mangrovei* . The table included the lipid detected in [g L^{-1}], as well as the lipid content in % (w/w).

Sample	Lipid [g L^{-1}]	Lipid [%]
Fermentation 5	3,15	60
Fermentation 6	3,40	47
Fermentation 7	2,66	40
Airlift 3	7,71	46
Airlift 4	5,93	42
Airlift 6	10,94	46

4.5.2. Organic solvent selection

The cultures of *Schizochytrium mangrovei* cultivated in 300 mL shaking flasks were used to find the best organic solvent for a lipid extraction.

The approach with Hexane, Methanol, Petrol ether, rape seed oil, $CaCl_2$ and HCl did not extract the lipid of the microalgae. Here, the organic phase did not change its color and the culture phase did not change as well. The weighing of the organic phase resulted in hardly recognizable extracted lipids. The organic solvents that were able to extract the lipid can be seen in Table 24. Here, the organic phase changed it color to orange, the culture phase lost its turbidity. After centrifugation the cell debris was located at the bottom of the tube in form of a pellet. It is worth mentioning that only combinations of organic solvents were able to extract the lipid.

The lipid extraction process revealed the formation of a phase in between the organic solvent and the aqueous phase (liquid culture). This phase was present in each attempt to extract the lipid (Figure 33: Greiner tube with hexane as a lipid extraction

approach. Here, 3 phases were noticeable. The upper phase was clear followed by a dense, light pinkish phase. At the bottom of the tube the cell culture can be seen.).

Figure 33: Greiner tube with hexane as a lipid extraction approach. Here, 3 phases were noticeable. The upper phase was clear followed by a dense, light pinkish phase. At the bottom of the tube the cell culture can be seen.

Table 24: Lipid extraction results from *Schizochytrium mangrovei* . The table included the organic solvents used and the lipid extracted with the corresponding organic solvent.

Organic solvent	**Lipid [g L^{-1}]**
H_2SO_4 : Methanol : Petrol ether	7.240
Methanol : Hexane	7.670
Methanol : Petrol ether	7.415
Chloroform : Methanol : Water	8.415

The most lipid was extracted with a chloroform, methanol, and water mixture. Here, the organic phase gained the most intense orange color and 8.415 g of lipid have been extracted. The issue with this organic solvent mixture was that the organic phase was located at the bottom of the tube. Therefore, to isolate the organic phase the middle phase needed to be broken, which made it more difficult to gain a clean and clear organic phase without any impurities.

4.5.3. Lipid analysis

The lipid analysis of the extracted lipid did reveal the presence of DHA (38.81 %) as well as palmitic acid (50.65 %). EPA was not detected. Small amounts of other lipids were detected as well (Table 25): 2.40 % of myristic acid, 0.07 % of hexadecatrienoic acid, 3.06 % of stearic acid, 1.55 % of oleic acid, 0.06 % of vaccenic acid, 1.91 % of behenic acid and 0.47 % of docosadienoic acid.

Table 25: Lipid analysis of *Schizochytrium mangrovei.* The table showed the fatty acid composition of the extracted lipid including the percentage of their occurrence. The names of the fatty acids, their C-atom numbers and double bonds were mentioned.

Fatty acid	**C-atoms**	**Double bonds**	**lipid fraction [%]**
Myristic acid	14	0	2.40
Palmitic acid	16	0	50.65
Hexadecatrienoic acid	16	3	0.07
Stearic acids	18	0	3.06
Oleic acid	18	1n9	1.55
Vaccenic acid	18	1n7	0.06
Behenic acid	22	0	1.91
Docasadienoic acid	22	2n6	0.47
DHA	22	2n3	38.81

5. DISCUSSION

5.1. Microbiome study

The sequencing results showed a high similarity between the replicates of each samples. They are not identical, but overall the same organism groups are present in each replicate to a similar percentage (Figure 12). This is an indicator that the selected (micro-)habitats harbored similar microalgal communities. However, a difference was observed when the individual samples were compared to each other. Especially the samples 3B, 3C, 3D show a different microbiome composition compared to the others, with a high percentage of SAR present in them. SAR is a superkingdom consisting of Stramenopiles, Alveolate and Rhizaria (Stephenson & Rojas, 2017). The superkingdom SAR is also associated with the microbiome of sponges. Rodriguez-Marconi et al. (2015) found a high occurrence of SAR in Antarctic sponges. SAR has also been found as a main component of the microbiome of an Acid Mine Drainage (Mesa et al., 2017). Samples 1A and 1B are similar to 2A, 2B and 2C. This can be explained by the location of the samples. The two locations where the samples have been taken are very close to each other and from similar altitudes. Samples 3A, B, C, D and E have been taken at completely different locations. Samples Garten and Pool are both non-natural habitats of microalgae. Those samples appear similar regarding the eukaryotic microorganisms in them. Most abundant organisms on phylum level were *Archaesplastida, Opisthokonta* and SAR.

A comparison of the locations supports the aforementioned assertions (Figure 13). A high similarity of the samples from Triebener Tauern and Drei Lacken as well as Graz and Ennstal could be observed, where Graz and Ennstal showed the highest similarities. They have the common factor of human influence, which might lead to a similar microbiome. The study of Tyakht and colleagues (2014) on the rural and urban microbiota obtained similar results regarding the comparable microbiome of different cities and villages. Here, the microbiome of the investigated urban location were associated with microbes linked to human health. The microbiome found in rural areas showed significant differences compared to the urban habitats. The samples from Graz and Ennstal were both taken from red-brown spots on a plastic chair and a pool tile, which is a factor shared by both samples. The location Triebener Tauern and Drei Lacken are geographically near to each other and the samples have been taken at similar altitudes, which might explain the similarity of the samples originating from these two locations. However, Drei Lacken showed more diversity than Triebener Tauern, while the

location Seetaler Alpen exhibited the highest microbial diversity. Overall, *Chloroplastida* and *Nucletmycea* were the two most abundant microorganisms. Henson and colleagues (2018) also found a high percentage of *Nucletmycea* when they analyzed river water. In this work, samples from the Mississippi River were taken and analyzed. *Nucletmycea* were identified as part of the core microbiome of the river samples.

A similar picture presented itself by comparison of the snowfield samples (Figure 14). The snowfield samples 1A and 1B come from the same location and showed high similarities between each other compared to the snowfield samples 3A, 3D and 3E. The snowfield samples 3A, 3D and 3E themselves were very similar to each other with a very high percentage of *fungi*. The similarity of the snowfield samples 1A and 1B as well as the similarity of the snowfield samples 3A, 3D and 3E can again be explained by the location of the sample taking. The samples similar to each other have been taken from different snowfields at the same location. The snowfield sample 3D showed the highest abundance of microorganisms of all snowfield samples. Most present were fungi and *Chlorophyta* on the taxonomical order level.

In the water samples, substantial differences were observed (Figure 15). Each sample shows a very specific composition of the eukaryotic community. The samples lake2A and lake2B were the most similar out of all the water samples. This can be explained by sampling location. Sample lake2C is taken from a swimming pond, whereas samples from lake2A and lake2B were not. This might explain the difference within the samples lake2C and lake2A/2B. The influence of humans, e.g. by swimming, might change the microbiome of the lake and therefore lead to a different composition of eukaryotic microorganisms. However, the other water samples did not show any significant similarities, even though they have been taken from the same location. This could be a result of the types of water the samples have been taken from. Typically *Actinobacteria* and *Alphaproteobacteria* are found in freshwater samples, as observed by Llirós et al. (2014). The composition can be regulated by changing nutrient content in the water, the pH value of the freshwater and the temperature (Llirós et al., 2014).

When comparing the samples from the chair and the tile pool samples high similarities (Figure 16) could be observed. Both sample locations have a high impact of humanity and are not traditional natural habitats of microalgae. Even though the location of the samples is not the same (Graz and Ennstal), the eukaryotic organisms that have been found are similar. *Chlorophyta* was detected as the most abundant microorganism.

The PCOA plot showed the similarity of the samples (Figure 18). Snowfield samples 1A showed a high similarity, expect for two replicates, which were more similar to snowfield samples 1B. This can be explained by the different color of the snowfields where the samples were taken. Snowfield samples 1B was taken from a green snowfield. The snowfield of samples 1A was differently colored. The two samples, which are closer to snowfield sample 1B, were taken from a greener area of the snowfield, whereas the other samples were taken from a red part of the snowfield. The samples from the plastic chair were very similar to each other as well as the samples from the tile of a pool. The two non-natural habitats showed a high similarity on the PCOA plot. The water samples were very similar to each other, independent of the location. The mixing of the water phase might explain these similarities. In a water medium, which is well mixed, the population is spread more evenly compared to e.g. snowfields, where no mixing takes place. The snowfield samples 3A, 3D and 3E were located near to each other. Overall the PCOA plot supported the information gained from the bar charts. It also pointed out a high similarity of two replicates of samples snowfield1A with snowfield samples 1B, which was not that clear from the bar charts. Also the similarity from the water samples was made clearer.

Generally, the microbiome study revealed a high similarity of the water samples independent of the sampling location while for the snowfields the coloring of the snowfields seemed to have a high impact on the composition of the occurring microorganism.

5.2. Heterotrophic growth experiments

The experiments with different substrate concentrations revealed for *Chlorella vulgaris* an ideal substrate concentration of 40-60 g L^{-1} glucose. Even though the calculated values for the key indicators were the highest for 60 g L^{-1} glucose, the growth curve exhibited the best behavior for the 40 g L^{-1} glucose. Here, the lag phase at the beginning of the cultivation was the shortest, followed by an immediate exponential phase. The cultivation with 60 g L^{-1} glucose displayed a lag phase that was longer than for the 40 g L^{-1} glucose cultivation. In both cases the entire glucose was used up and no inhibitory effects on the algal growth were indicated. The cultivation with 80 g L^{-1} glucose clearly showed that higher substrate concentrations inhibit the growth of the microalgae. This statement is supported by the calculated key indicator values. The approach with the highest glucose concentration lead to the lowest biomass concentration as well as the lowest growth rate, biomass productivity and yield. This cultivation approach ended with glucose present in the flask. The algal culture was not able to use up the substrate within 180 hours. In comparison to the lower substrate concentration approach: Here, the entire glucose was used up after approximately 150 hours. Similar results were documented by

Doucha (2011). The fermentation of the microalgae with 40 g L^{-1} glucose as a substrate resulted in a similar biomass concentration. However, mentioned in his work is that fedbatch cultivation can reach even higher biomass concentrations. With fedbatch fermentations, biomass concentration of 48 g L^{-1} are documented (Shi & Chen, 2008).

The results gained here resulted in the usage of 40 g L^{-1} for the fermentation process of *Chlorella vulgaris*.

For *Schizochytrium mangrovei* two different medium components were tested. The flask experiments for the nitrogen source revealed that the growth *of Schizochytrium mangrovei* on $(NH_4)_2SO_4$ was not possible. The uptake of $(NH_4)_2SO_4$ resulted in the release of protons from the algae into the medium (Eustance E. et al., 2013), which decreased the pH to a value were the microalgal culture could not survive. Even though the medium for the flask experiments contained a puffer, it was not possible to puffer the pH change due to the cultivation with $(NH_4)_2SO_4$. The cultivation with Urea showed a slight decrease in the pH value, which did not have a high impact on the culture. Due to the cell death in the cultivation with $(NH_4)_2SO_4$, the cultivation with Urea created the highest biomass concentration, growth rate, biomass productivity and yield. For the substrate cultivation experiment the cultivation of urea was preferred.

Schizochytrium sp. are reported to be able to work with very high glucose concentrations (up to 150 g L^{-1}) (Yaguchi et al., 1997). This report was not support by the work conducted in this thesis. The cultivation of *Schizochytrium mangrovei* with glucose concentrations of 40 – 60 g L^{-1} created the best growth curves. In both cases a very short lag phase was followed by a rapid increase in biomass. The 40 g L^{-1} glucose cultivation ended after 50 hours with no glucose present, whereas the 60 g L^{-1} glucose cultivation took 70 hours and ended with 8 g L^{-1} glucose remaining. The cultivation with a higher substrate concentration of 80 g L^{-1} glucose also exhibited a different growth behavior. The starting point of the exponential phase was later compared to the lower substrate concentration. The culture was not able to use the entire glucose. After 70 hours, 30 g L^{-1} glucose were still present and the growth rate declined. A slight inhibitory effect was observed. Due to the reported high glucose tolerance the cultivation with 120 g L^{-1} glucose was performed. This cultivation approach showed a strong inhibitory effect of the substrate to the microalgae. The cultivation was performed for 350 hours. Within this time the algae used up the glucose very slowly. *Schizochytrium mangrovei* was not able to use up the entire glucose provided. A look at the biomass concentration revealed a rather high concentration, but the time needed for creation of this biomass relativizes the result. The highest

biomass concentration was produced with 60 g L^{-1} glucose. The highest biomass productivity was calculated for the 40 g L^{-1} glucose cultivation.

Therefore, for the batch fermentation 40 g L^{-1} glucose and 30 mM Urea were used.

5.3. Batch fermentation

During the three fermentations with *Chlorella vulgaris* the regulation cascade of the oxygen saturation was shown to be the most important factor. The first fermentation, where the pO_2 cascade was stirrer [100-1500 rpm] – flow [2-10 NL min^{-1}] – pressure [0-1 bar], the microscopy revealed a high number of destroyed cells. Due to the high stirrer activity (up to 1000 rpm) high shear forces were created. It is very likely that the sensitive microalgal cells did not endure the high shear forces and that therefore biomass was lost during the fermentation. This would explain the lower biomass concentration in the fermenter compared to the shaking flask. For the next fermentation attempt the pO_2 regulation cascade was changed to flow [2-10 NL min^{-1}] – pressure [0-1 bar] – stirrer [100-500 rpm]. The change in the regulation cascade resulted in a similar biomass concentration. Here the glucose was not entirely consumed. The regulation cascade was completely exhausted and the pO_2 value sank after hour 40. That might be the reason why the glucose was not used up entirely. The culture was under oxygen limitation and was not able to grow any further. However, the biomass concentration reached after 40 hours was the same as for the first fermentation attempt. If the oxygen limitation would not have been present during the fermentation, probably a much higher biomass concentration than in the first fermentation could have been achieved. For the third fermentation the regulation cascade was changed again: flow [2-10 NL min^{-1}] – pressure [0-1.5 bar] – stirrer [100-500 rpm]. The stirrer speed was not increased due to the experiences with the higher stirrer activity from the first fermentation. Instead the pressure, which was able to build up in the fermenter, was regulated higher. The third fermentation unfortunately ended prematurely due to the leakage of the acid pump tube. Due to the open system and the unsterile conditions, the data from this fermentation was not usable for analysis.

The fermentation of *Schizochytrium mangrovei* created some challenges. The first fermentation showed a very low biomass concentration. The behavior of the microalgae differed extremely from the shaking flask experiment to the fermenter experiment. After the first fermentation attempt the growth of the microalgae seemed inhibited. Due to the experience gained from the *Chlorella vulgaris* fermentation the initial thought was that the issue could be the oxygen saturation. Consequently, for the second fermentation the pO_2 regulation cascade was changed, but no significant improvements were observed. The same issue occurred for the third

fermentation. Evidently, a change in the pO_2 regulation did not influence the outcome of the fermentation. In each fermentation the microalgae culture seemed to be inhibited. After intense analysis of the fermentation process the assumption was made that the issue might stem from a nutrient limitation. The sterilization of the fermenter including the medium was done at 121 °C for 30 min. Literature showed that Urea is heat sensitive and degrades before reaching its melting point (Rafat, 2014). If the microalgae did not have any or very little nitrogen, the growth would be inhibited due to the nutrition limitation. This assumptions needed to be investigated. Therefore the cultivation in 5 L airlift bioreactors was performed.

5.4. Airlift bioreactor experiments

The first step to confirm the theory of nutrient limitation was to simulate the fermentation experiment with the airlift bioreactor. When the medium was autoclaved twice to simulate the 121 °C for 30 min, similar key indicators as for the fermentation were observed. The fermenter simulation in the airlift bioreactor showed the same type of inhibition as the fermentation did. Enough oxygen was present in the airlift bioreactor and the culture was axenic. It grew, but only very slowly and the glucose concentration hardly sank.

The next step was to perform the same cultivation with sterile filtered medium to eliminate any effect of heat to the medium. In this experiment the growth curve looked differently. A higher biomass concentration was produced. The microalgae culture consumed all the glucose and grew. In the beginning, the cell growth was a little slower up until the point when the oxygen supply was increased. Even though the growth up until this point was slower compared to the shaking flask experiments, it still was better than in the fermenter. For the cultivation in the airlift bioreactor the controlling and regulation was not as good as it would be in a fermenter. This needs to be considered because the growth would be influenced by the bad conditions regardless of the nutrient limitation. When the oxygen supply for the culture was increased, the exponential phase started immediately and within 40 h the glucose was used up. With the results of those two experiments the initial assumption of the nutrient limitation during the fermentation was confirmed.

5.5. Lipid extractions and content analyses

The lipid of *Schizochytrium mangrovei* was extracted from the liquid culture because it was not possible to concentrate the biomass by centrifugation or filtration. This issue was first noticed with the flask experiments. The high lipid content of the microalgae might make it hard for the cells to settle. Regardless, the lipid extraction worked well with the liquid culture. To open the

cells they were homogenized. During the lipid extraction, a third phase in between the aqueous and organic phase formed. All attempts to get rid of this phase failed. A possible explanation could be that this third phase might be an accumulation of phospholipids, proteins, etc.. similar to an oil refinery's so-called gums. Different types or organic solvents are reported to work for the lipid extraction of *Schizochytrium mangrovei's* lipid (Choi et al., 2014 and Wang et al., 2015 and Yel et al., 2017). Many of the reported organic solvents did not work. Only organic solvents in combination with methanol had the ability to extract the lipid.

The lipid analysis of the extracted lipid revealed the presence of 38.81 % DHA in the lipid sample sent for analysis. *Thraustochytrids* are reported to be EPA and DHA producers (Lewis, Nichols & McMeekin, 1999). However, EPA was not found in a significant amount in the *Schizochytrium mangrovei* lipid extract. The composition of the lipid depends on the strain as well as the medium used. The absence of a significant amount of EPA does support research which suggest that *Schizochytrium mangrovei* is specifically interesting due to its high DHA content but not EPA content. (Fan et al., 2001).

6. CONCLUSIONS AND OUTLOOK

The present work provides novel insights into the ecology of microalgae and their industrial utilization. Next-generation sequencing was successfully applied to resolve algal community structures in different habitat. The microbiome study with different microalgal samples revealed that water samples have the most complex microbiome of all samples. However, they displayed the highest similarities independent of the sampling location. This might be caused by the movement and mixing of the water. The snowfield samples showed a higher similarity when taken at the same location. The coloring of the snowfield is indicative of a specific microbiome composition. The microbiomes of the urban habitats (pool tiles, plastic chair) were very similar even though the sampling location was not the same. In order to further refine the findings, more samples should be collected and analyzed in order to find all correlations between microbiome and sampling location, type of habitat (natural and artificial/urban) as well as the state of the water (liquid or snow/ice). The information gained from microbiome studies provides the means to identify microorganisms, which are able to support the growth of microalgae and hence improve their industrial application.

During the optimization of heterotrophic cultivation of two microalgae strains, important parameters for process improvements were defined. The heterotrophic cultivation of *Chlorella vulgaris* and *Schizochytrium mangrovei* showed that a glucose concentration of 40-60 g L^{-1} for *Chlorella vulgaris* and 40 g L^{-1} glucose for *Schizochytrium mangrovei* resulted in the best growth conditions for the microalgae. With these nutrient concentrations inhibiting effects on the microalgal growth can be excluded. Even though with other substrate concentrations occasionally higher key indicators (biomass concentration, yield, biomass productivity and growth rate) were achieved, the overall growth behavior of the microalgae was less optimized.

The controlled conditions during the cultivation in a fermenter improve the cultivation conditions and should therefore lead to a fast cultivation and higher key indicators than flask cultivation. With the SPV experiments it has been proven that *Schizochytrium mangrovei* has a high lipid content (~45%) with a high presence of DHA. To further improve the cultivation process, the fermentation should be optimized by utilizing different nitrogen sources to achieve a higher lipid content and DHA percentage. In this regard $(NH_4)_2SO_4$

could be used, as this nitrogen source reportedly improves the *Schizochytrium mangrovei* growth rate. To increase the key indicators different cultivation modes (e.g. fed-batch) should be tested for both microalgae.

Overall, microalgae become more important industrially and economically. Research in this field is increasing and necessary to enable the use of microalgae as a natural resource for pigments, vitamins, lipids and many more.

7. Chemicals

For the **medium and cultivation processes**, the following chemicals were used and purchased from:

Agar-Agar	Carl Roth, Karlsruhe, Germany
$CaCl_2 * 2 H_2O$	Carl Roth, Karlsruhe, Germany
H_3BO_3	Carl Roth, Karlsruhe, Germany
$CuSO_4 * 5 H_2O$	Carl Roth, Karlsruhe, Germany
$ZnSO_4 * 7 H_2O$	Carl Roth, Karlsruhe, Germany
$CoSO_4 * 7 H_2O$	Carl Roth, Karlsruhe, Germany
$MnCl_2 * 4 H_2O$	Carl Roth, Karlsruhe, Germany
$(NH_4)6Mo7O_{24} * 4 H_2O$	Carl Roth, Karlsruhe, Germany
$MgSO_4*7H_2O$	Carl Roth, Karlsruhe, Germany
Glucose	Carl Roth, Karlsruhe, Germany
NaOH	Carl Roth, Karlsruhe, Germany
HCl	Carl Roth, Karlsruhe, Germany
NaCl	Carl Roth, Karlsruhe, Germany
$MgCl_2 * 6 H_2O$	Carl Roth, Karlsruhe, Germany
KCl	Carl Roth, Karlsruhe, Germany
$NaNO_3$	Carl Roth, Karlsruhe, Germany
$MgSO_4 * 7 H_2O$	Carl Roth, Karlsruhe, Germany
$CaCl_2 * 2 H_2O$	Carl Roth, Karlsruhe, Germany
MOPS-Puffer	Carl Roth, Karlsruhe, Germany
Citric acid monohydrate	Carl Roth, Karlsruhe, Germany
Ferric ammonium citrate	Carl Roth, Karlsruhe, Germany
$Na_2EDTA * 2 H_2O$	Carl Roth, Karlsruhe, Germany
Na_2CO_3	Carl Roth, Karlsruhe, Germany
K_2HPO_4	Carl Roth, Karlsruhe, Germany
$Na_2MoO_4 * 2 H_2O$	Carl Roth, Karlsruhe, Germany
Vitamin B12	Carl Roth, Karlsruhe, Germany
Biotin	Carl Roth, Karlsruhe, Germany

Thiamin HCl	Carl Roth, Karlsruhe, Germany
Urea	Carl Roth, Karlsruhe, Germany
$(NH_4)_2SO_4$	Carl Roth, Karlsruhe, Germany
Yeast extract	Carl Roth, Karlsruhe, Germany
Peptone	Carl Roth, Karlsruhe, Germany
$MgSO_4$	Carl Roth, Karlsruhe, Germany
Glanapon2000	Carl Roth, Karlsruhe, Germany
Ethanol (70%)	Carl Roth, Karlsruhe, Germany

For the **DNS-assay** the following chemicals were utilized and purchased from:

3,5-dinitro-salycilic acid	Sigma-Aldrich, Darmstadt, Germany
Potassium Sodium tartrate	Sigma-Aldrich, Darmstadt, Germany

For the **SPV-assay** the following chemicals were utilized and purchased from:

Vanillin	Sigma-Aldrich, Darmstadt, Germany
Phosphoric acid (85%)	Carl Roth, Karlsruhe, Germany
Sulfuric acid (97%)	Carl Roth, Karlsruhe, Germany
Ethanol (99,9%)	Sigma-Aldrich, Darmstadt, Germany

For the **lipid extraction** experiments the following chemicals were utilized and purchased from:

Hexane	Carl Roth, Karlsruhe, Germany
Methanol	Carl Roth, Karlsruhe, Germany
Petrol ether	Carl Roth, Karlsruhe, Germany
H_2SO_4	Carl Roth, Karlsruhe, Germany
Chloroform	Carl Roth, Karlsruhe, Germany

8. References

Aguiar-Pulido, V. (2016). Metagenomics, Metatranscriptomics, and Metabolomics Approaches for Microbiome Analysis. *Evolutionary Bioinformatics Online*.

Benne, R. M., Honda, D., Beakes, G. W., & Thines, M. T. (2017). Labyrinthulomycota. In A. G. John M. Archibald, *Handbook of the Protists* (pp. 507-542). Springer.

Berg, G., Grube, M., Schloter, M., & Smalla, K. (2014). The plant microbiome and its importane for plant and human health. *Frontiers in Microbiology*.

Beyerinck, M. W. (1890). Culturversuche mit Zoochlorellen, Lichenengonidien und anderen niederen Algen. *Botanische Zeitung*, 726-740.

Bitog, J., Lee, I.-B., Lee, C.-G., Kim, K.-S., Hwang, H.-S., Hong, S.-W., . . . Mostafa, E. (2010). Application of computational fluid dynamics for modeling and designing photobioreactors for microalgae production: A review. *Computers and Electronics in Agriculture*, 131-147.

Callahan, B. J., McMurdie, P. J., Rosen, M. J., Han, A. W., Johnson, A. J., & Holmes, S. P. (2016). DADA2: High resolution sample inference from Illumina amplicon data. *Nature Methods*, 581-583.

Caporaso, G. J., Kuczynski, J., Stombaugh, J., Bittinger, K., Bushman, F. D., Costello, E. K., . . . Knight, R. (2010). QIIME allows analysis of high-throughput community sequencing data. *Natura Methods*, 335-336.

Chen, Liu, J., & Feng. (2016). Biology and Industrial Applications of Chlorella: Advances and Prospects. In S. R. Clemens Posten, *Microalgae Biotechnology* (pp. 1-24). Springer.

Chodchoey, K., & Verduyn, C. (2012). Growth, fatty acid profile in major lipid classes and lipid fluidity of Aurantiochytrium mangrovei SK-02 as a function of growth temperature. *Brazil Journal of Microbiology*, 187-200.

Choi, S.-A., Jung, J.-Y., Kim, K., Lee, J.-S., Kwon, J.-H. K., Yang, Y.-W., & Park, Y.-J. (2014). Acid-catalizes hot-water extraction of dodsahexaenoic acid (DHA)-rich lipids from Autantiochytrium sp. KRS101. *Bioresource Technology*, 169-472.

Day, J. G., Gong, Y., & Hu, Q. (2017). Microoplanktonic grazers - A potentially devastating threat tot the commerical success of microalgal mass culture. *Algal Research*, 356-365.

Dayal, R. (1996). *Advances in Zoosporic Fungi.* M.D. Publications.

Doucha, J. (2011). Production of high-density Chlorella culture grown in fermenters. *Journal of Applied Phycology*.

Dyall, S. C. (2015). Long-chain omega- 3 fatty acids and the brain: a review of the independent and shared effects of EPA, DPA and DHA. *Frontiers in aging neuroscience*, 7-52.

Dyall, S. C. (2015). Long-chain omega-3 fatty acids and the brain: a review of the independent and shared effects of EPA, DPA and DHA. *frontiers in aging neuroscience*, 7-52.

Dyall, S. C., & Michael-Titus, A. T. (2008). Neurological Benefits of Omega-3 Fatty Acids. *Neuromolecular Medicine*, 219-235.

Eustance, E., Gardner, R. D., & Peyton, B. M. (n.d.). Growth, nitrogen utilizatioin and biodiesel potential for z chlorophytes grown on ammonium, nitrate or urea.

Eustance, E., Gardner, R. D., Moll, K., & Peyton, B. M. (2013). Growth, nitrogen utilization and biodiesel potential for two chlorophytes grown on ammoniu,. nitrate or urea. *Journal of applied Phycology*.

Fan, K., Chen, F., Jones, E., & Vrijmoed, L. (2001). Eicosapentaenoic and docosahecaenoic acids production by and okara-utilizing potential of thaustochytrids. *Journal of Industrail Microbiology & Biotechnology*, 199-202.

Graham, L. E., & Wilcox, L. W. (2015). Why we need more algal metagenomes. *Journal Phycology*, 1029-1036.

Grossman, A. (2016). Nutrient Acquisition: The Generation of Bioactive Vitamin B12 by Microalgae. *Current Biology*, 319-337.

Gupta, A., Singh, D., Byreddy, A. R., Thyagarajan, T., Sonkar, S. P., Mathur, A. S., . . . Puri, M. (2016). Exploring omega-3 fatty acids, enzymes and biodiesel producing thraustochytrids from Australian and Indian marine biodiversity. *Biotechnology Journal*, 345-355.

Henson, M., Hanssen, J., Spooner, G., Fleming, P., Pukonen, M., Stahr, F., & Thrash, J. C. (2018). Nutrient dynamics and stream order influence microbial community patters

along a 2941 kilometer transect of the Mississippi River: Microbial regime changes on the Mississippi River. *Li,nology and Oceanography*, 1-19.

Hong, D. D., Nhat, P. V., & Ahn, H. T. (2016). Characteristic of cell morphology in different stages of schizochytrium mangroevi PQ6´s life cycle. *Tap chi sinh hoc journal of biology*.

Hu, J., Nagarajan, D., Zhang, Q., Chang, J.-S., & Lee, D.-J. (2018). Heterotrophic cultivation of microalgae for pigment production: A review. *Biotechnology Advances*, 54-67.

Khan, M. I., Shin, J. H., & Kim, J. D. (2018). The promising future of microalgae: current status, challenges, and optimization of a sustainable and renewable industry for biofuels, feed, and other products. *Microbial Cell Factories*.

Knight, J. A., & Anderson, S. R. (1972). Chemical Basis of the Sulfo-phopho-vanillin Reaction for Estimating Total Serum Lipids. *Clinical Chemistry*.

Kumusha, A., Selvakumar, S., Dilshad, P., Vaidayanathan, G., Thakur, M., & Sarada, R. (2010). Methylcobalamin--a form of vitamin B12 identified and characterised in Chlorella vulgaris. *Food Chemistry*.

Lewis, T. E., Nichols, P. D., & McMeekin, T. A. (1999). The Biotechnolgical Potential of Thraustochytrids. *Marine Biotechnology*, 580-587.

Leyland, B., Leu, S., & Boussiba, S. (2017). Are Thraustochytrids algae? *Fungal Biology*, 835-840.

Liu, J., Sun, Z., & Chun, F. (2014). Heterotrophic Production of Algal Oils. In *Biofuels from Algae* (pp. 111-142). Elsevier.

Llirós, M., Inceoğlu, Ö., Garcia-Armisen, T., Anzil, A., Leporcq, B., Pigneur, L.-M., . . . Servais, P. (2014). Bacterial Community Composition in Three Freshwater Reservoirs of Different Alkalinity and Trophic Statur. *PLOS Journals*.

Lozupone, C., & Knight, R. (2005). UniFrac: a New Ohylogenetic Method for Comparing Microbial Communities. *Applied and Environmentall Microbiology* .

Mesa, V., Gallego, J. L., Gonzalez-Gil, R. L., Sanchez, J., Mendez-Garcia, C., & Pelaez, A. I. (2017). Bacterial, Archaeal, and Eukaryotic Diversity across Distinct Microhabitats in an Acid Mine Drainage. *Frontiers in Microbioloy*.

Mohan, S. V., Devi, M. P., Venkata, S. G., & Chandra, R. (2014). Algae Oils as Fuels. In *Biofuels from Algae* (pp. 155-187). Elsevier.

Morales-Sanches, D., Martines-Rodriguez, O. A., & Martinez, A. (2016). Heterotrophic cultivation of microalgae: production of metabolites of commercial interest. *Journal of Chemical Technology and Biotechnology*.

Mühlroth, A., Li, K., Rokke, G., Winge, P., & Yngvar Olsen, M. F.-M. (2013). Pathway of Lipid Metabolism in MArine Algae, Co-Expression Network, Bottlenecks and Candidate Genes for Enhanced Production of EPA and DHA in Species of Chromista. *Marine Drugs*, 4662-4697.

Müller, H.-J., & Prange, D. R. (2016). *PCR - Polymerase - Kettenreation.* Springer Spektrum.

Palz, O. (2001). Photobioreactors: production systems for phototrophic microorganisms. *Applied Microbiology and Biotechnology*.

Priyadarshani, I., & Rath, B. (2012). Commercial and industrial applications of micro algae - A review. *Journal of Algal Biomass Utilization*, 89-100.

Pulz, O., & Gross, W. (2004). Valuable products from biotechnology of microalgae. *Applied Microbiology and Biotechnology*, 635-648.

Rafat, F. (2014). Effect of different heating rate on the thermal decomposition of urea in an opren rection vessel. *Archievs of Applied Science Research*, 75-78.

Rappel, R. (2013). "Docosahexaenoic Acid Production by the Thraustochytrid Aurantiochytrium Limacinum SR21 Using Various Carbon Sources. *Diploma Thesis*.

Rische, T. (2015). Potential lipid and glycogen accumulations under heterotrophic growth conditions within the thermo.acidophilic red microalgae galdieria sulphuraria. *Master Thesis*.

Rodriguez-Marconi, S., De la lglesia, R., Diez, B., Fonsenca, C. A., Hajdu, E., & Trefault, N. (2015). Characterization of Bacterial, Archaeal and Eukaryote Symbionts from Antarctic Sponges Reveals a High Diversity at a Three-Domain Level and a Particular Signature for This Ecosystem. *PLOS One*.

Rognes, T., Flouri, R., Nichols, B., Quince, C., & Mahe, R. (2016). VSEARCH: a versatile open source tool for metagenomics. *PeerJ*.

Russell, J. A. (2014). Nature´s microbiome: introdcution. *Molecular Ecology*, 1225-1237.

Safi, C., Zebib, B., Merah, O., Pontalier, P.-Y., & Vaca-Garcia, C. (2014). Morphology, composition, production, processing and applications of Chlorella vulgaris: A review. *Renewable and Sustainable Energy Reviews*, 265-278.

Sahin, D., Tas, E., & Altindag, U. H. (2018). Enhancement of docosahexaenoic acid (DHA) production from Schizochytrium sp. S31 using different growth medium conditions. *AMB Express*.

Shen, X.-F., Chu, F.-F., Lam, P. K., & Zeng, R. J. (2015). Biosynthesis of high yield fatty acids from Chlorella vulgaris NIES-227 under nitrogen starvation stress during heterotrophic cultivation. *Water Research*, 294-300.

Shi, X.-M., & Chen, F. (2008). High-Yield Production of Lutein by the green microalgae Chlorella protothecuides in heterotrophic fed-batch culture. *Biotechnology Progress*.

Singh, J., & Saxena, R. C. (2015). An Introduction to Microalgae: Diversity and Significance. In P. S.-K. Kim, *Handbook of Marine Microalgae* (pp. 11-14). Elsevier.

Stal, L. J., & Cretoiu, M. S. (2016). *The Marine Microbiome: An Untapped Source of Biodiversity and Biotechnological Potential.* Springer.

Stephenson, S. L., & Rojas, C. (2017). *Myxomycetes: Biology, Systematics, Biogeography, and Ecology*. Elsevier Inc.

Sunagawa, S., Mende, D., Zeller, G., Izquierdo-Carrasco, F., Berger, S., Kultima, J., . . . Bork, P. (2013). Metagenomic species profiling using universal phylogenetic marker genes. *Nature Methods*.

Terashima, M., Umezawa, K., Mori, S., Kojima, H., & Fukui, M. (2017). Microbial Community Analysis of Colored Snow from an Alpine Snowfield in Norther Japan Reveals the Prevalance of Betaproteiacteria with Snow Algae. *Frontiers in Microbiology*.

Thomas, T., Gilbert, J., & Meyer, F. (2012). Metagenomics - a guide from sampling to data analysis. *Microbial informatics and experimentation*.

Toledo, V. d., Ruvolo-Takasusuki, M. C., Oliveira, A. J., Chambó, E. D., & Lopes, S. M. (2012). *Spectrophotometry as a Tool for Dosage Sugars in Nectar of Crops Pollinated by Honeybees.* InTech.

Turnbaugh, P. J., Ruth, L. E., Hamady, M., Fraser-Liggett, C. M., Knight, R., & Gordon, J. I. (2007). The Human Microbiome Project. *Nature*, 804-810.

Tyakht, A. V., Alexeev, D. G., Popenko, A. S., Kostryukova, E. S., & Govorun, V. M. (2014). Rural and urban microbiota. *Gut Microbes*, 351-356.

Wang, H., Klinthong, W., Yang, T., & Tan, C. (2015). Continous extraction of lipids from Schizochytrium sp. by CO2-expanded ethanol. *Bioresource Technology*, 162-168.

Wells, M. L., Potin, P., Ctraigie, H. S., Taven, J. A., Merchant, S. S., Helliwell, K. E., . . . Brawley, S. H. (2017). Algae as nutrional and functional food sources: revisistin our understanding. *Journal of Applied Phycology*, 949-970.

Yaguchi, T., Tanaka, S., Yokochi, T., Nakahara, T., & Higashihara, T. (1997). Production of High Yields of Docosahexanoic Acid by Schizochytrium sp. Strain SR21. *Journal of the American Oild Chemists´ Society*, 1431-1434.

Yel, N. C., Yekbiga, E., Tüter, M., & Karagüler, N. G. (2017). Comparison of Cell Disruption and Lipid Extraction Methods for Improving Lipid Content of Schizochytrium sp. S31. *Journal of Molecular Biology and Biotechnology*, 9-12.

9. Table of Figures

10. Table of Tables